Soil Biology and Biochemistry 221 (2026) 110241

Contents lists available at ScienceDirect

Soil Biology and Biochemistry

journal homepage: www.elsevier.com/locate/soilbio

Visualizing soil chemical heterogeneity in time and space using optical sensors: advances, challenges, and prospects

Pauline Sophie Rummel [a,b], Ya Jie Knöbl [a], Martin Reinhard Rasmussen [a,c], Klaus Koren [a,*], Andrey V. Kalinichev [a,d]

[a] Department of Biology, Section for Microbiology, Aarhus University, Ny Munkegade 116, Aarhus C, 8000, Denmark
[b] Centre for Environmental Sciences, Hasselt University, Agoralaan Building D, Diepenbeek, 3590, Belgium
[c] Pioneer Center Land-CRAFT, Department of Agroecology, Aarhus University, Ole Worms Allé 3, Aarhus, 8000, Denmark
[d] Aarhus Institute of Advanced Studies, Aarhus University, Høegh-Guldbergs Gade 6B, Aarhus C, 8000, Denmark

ARTICLE INFO

Keywords:
Planar optodes
Chemical imaging
Soil biogeochemistry
Microenvironments
Rhizosphere
Oxygen dynamics

ABSTRACT

Understanding how soil biogeochemical processes develop from microscale heterogeneity remains a central challenge in soil science. Many key transformations, including microbial respiration, nutrient cycling, and greenhouse gas production, occur in spatially structured microenvironments that are difficult to capture with conventional bulk measurements. Planar optodes have emerged as a powerful tool to address this challenge by enabling two-dimensional imaging of chemical parameters such as oxygen (O_2), pH, ammonia (NH_3), and carbon dioxide (CO_2) across soil profiles with high spatial and temporal resolution.

In this Perspective, we critically examine what planar optodes can reveal about soil biogeochemistry and what they cannot. We discuss the sensing principles underlying optode measurements and review recent applications that use optode imaging to visualize redox heterogeneity, rhizosphere processes, and biogeochemical hotspots that remain invisible to conventional approaches. These observations provide a dynamic view of soil chemistry and open new opportunities to generate mechanistic hypotheses about the controls of microbial activity and nutrient transformations. Particular emphasis is placed on the strengths of optodes for identifying microsites and guiding targeted sampling strategies.

At the same time, we highlight key limitations, including challenges related to calibration, optical artefacts, and the interpretation of two-dimensional concentration fields in inherently three-dimensional soil systems. We also discuss how optode imaging can be integrated with complementary techniques such as microsensors, molecular analyses, gas flux measurements, and structural imaging to better resolve links between soil structure and biogeochemical processes.

Finally, we outline emerging directions that could expand the role of optodes in soil research, including their integration with data-driven and process-based models. Used thoughtfully and in combination with other approaches, planar optodes can become a central tool for investigating soil biogeochemistry at the microscale.

1. Introduction

Soils are a complex mixture of mineral particles, organic matter, water, and gases, combining three stages of matter (solid, liquid, gas). In addition to physical soil structure, biochemical parameters such as soil organic matter (SOM), nutrient availability, and pH deviate strongly over small distances. Furthermore, biological factors like plant roots and soil (micro-) organisms add to the small-scale complexity of soils. Due to its impact on soil processes, elucidating spatial heterogeneity of soil parameters on small-to micro-scales is becoming increasingly important. Yet, many methods to analyze soil physical and biochemical parameters are limited to destructive one-point measurements that cannot capture temporal and spatial heterogeneity.

Both chemical and biological processes in soil vary along with these small-scale gradients of physical and biochemical parameters. The distribution of soil microorganisms largely depends on the availability of their main substrates, leading to distinct communities driving nutrient turnover processes in soil (Franklin and Mills, 2009). For instance, SOM

* Corresponding author.
E-mail address: klaus.koren@bio.au.dk (K. Koren).

https://doi.org/10.1016/j.soilbio.2026.110241
Received 20 March 2026; Received in revised form 24 June 2026; Accepted 6 July 2026
Available online 8 July 2026

distribution and C turnover processes depend on soil texture, moisture, and O_2 availability, affecting C losses as well as C sequestration (Angst et al., 2021; Schlüter et al., 2022). Favorable conditions initiate the formation of microbial hotspots with up to 20-times higher microbial activity and respiration, leading to increased O_2 consumption and CO_2 production (Kuzyakov and Blagodatskaya, 2015). Small-scale O_2 distribution is thus a crucial parameter determining where aerobic or anaerobic processes dominate. Soil pH is another main factor controlling bacterial communities and their functions (Wang et al., 2019). Within a soil profile, pH can vary substantially throughout the soil profile depending on SOM and carbonate distribution, root exudation, and soil management, such as liming and fertilization. Spatial heterogeneity of N turnover processes depends strongly on the aforementioned parameters (O_2, SOM/C, pH). For instance, while nitrification is mostly carried out by autotrophic aerobic bacteria and archaea, denitrifying microorganisms require a C source and anoxic conditions (Butterbach-Bahl et al., 2013).

A multitude of analytical methods and techniques have been developed to analyze soil physical, chemical, and biological parameters. Mostly, bulk soil parameters are analyzed, often requiring large amounts of soil to be accurate and representative. Normally, samples are collected from the field or experiment and taken to the lab, where they need to be processed before the desired parameters can be analyzed, including steps like drying, sieving, and/or extractions with water or salt solutions. For other parameters, such as bulk density, soil pore space (distribution), water holding properties, etc., undisturbed samples are needed. All these sampling and analysis techniques have in common that they're destructive and do not allow for repeated measurements or time series. In contrast to destructive soil sampling, some parameters can be directly non-destructively measured in the field, including soil moisture, temperature, electric conductivity, pH, and some nutrients (i.e., NO_3^-, P, K) allowing for continuous monitoring (Thomson et al., 2012; Susha Lekshmi et al., 2014; Potdar et al., 2021; Ameer et al., 2024). However, these measurements are normally restricted to single points or small soil volumes, not reflecting the spatial heterogeneity.

To capture two-dimensional (2D) spatial heterogeneity, different methods have been developed, including Diffusive Gradients in Thin Films (DGT, (Liu et al., 2024), zymography (Spohn et al., 2013; Heitkötter and Marschner, 2018), and planar optodes (Li et al., 2019). DGT gels are available for a multitude of parameters, including cationic metals, nitrate, phosphate, and other oxyanions, antibiotics, bisphenols, and nanoparticles (Santner et al., 2015). Zymography can be utilized to analyze the distribution of enzyme activities in soil, including, for example, β-glucosidase, phosphatase, and chitinase (Spohn et al., 2013; Razavi et al., 2019). Both these methods are single-use only. Thus, for each point in a time series, a new DGT or zymography gel must be applied to the desired soil surface, causing interference and disturbance of the soil profile. The only 3D method currently available to determine soil spatial heterogeneity is X-ray μCT. It allows for capturing the three-dimensional distribution of soil matrix, water, air, and (to a certain extent) particulate organic matter (POM) or plant roots (Helliwell et al., 2013).

Planar optodes are the only method that facilitates the determination and monitoring of in-situ spatial heterogeneity of soil chemical parameters (i.e., O_2, CO_2, pH) over time. Planar optodes are 2D sensor foils that normally consist of an indicator dye embedded in a polymer, which reversibly interacts with the desired parameter (see details in Chapter 2). Relevant applications in soils include the determination of O_2, pH, CO_2, NH_3, and temperature. This perspective article aims to present a critical assessment of planar optodes for soils, highlighting applications, limitations, and future directions.

2. What are planar optodes?

2.1. Operating principle: imaging, dyes, calibration

Planar optodes are a 2D imaging technique that can be applied to investigate biogeochemical processes at a high spatial and temporal resolution in heterogeneous sediments and soils (Li et al., 2019). A planar optode consists of sensing chemistry (an analyte-responsive luminophore or dye), which is immobilized in a thin polymer matrix and usually coated onto a flexible plastic or glass substrate. When the target analyte (e.g., O_2, H^+ for pH, NH_3, CO_2; ionic species such as NH_4^+, K^+, Na^+, Ca^{2+}, etc.) interacts with the sensor dye, it induces a change in the optical properties of the dye, typically a change in fluorescence intensity or lifetime, or a color shift. This change can then be quantitatively related to the analyte concentration via calibration. In practice, the planar optode is placed in contact with the soil sample, and a camera equipped with appropriate excitation light sources (for a luminescence mode) and filters is used to capture images of the optode's luminescence or color (Fig. 1). By capturing the optical signal across the entire optode, a 2D map of analyte concentration is obtained over the area of interest. Advanced imaging setups may employ ratiometric techniques (comparing two wavelengths), lifetime imaging, or hyperspectral imaging to achieve more robust, reference-calibrated results. The result is a pseudocolor image where each pixel corresponds to the local level (i.e., concentration) of the measured parameter (chemical species, i.e., O_2, H^+, etc.), at spatial resolutions down to several μm in optimized systems.

The "standard" planar optode is fabricated from a "sensor cocktail" containing the indicator dye for the reversible detection of the analyte and a reference dye to enable ratiometric measurement, both dissolved in an appropriate polymer solution. This cocktail is thinly applied to a flat, transparent surface made of sturdy plastics like PET foils or glass using techniques such as knife coating, drop casting, or spin coating (Moβhammer et al., 2019). After evaporation of the solvent, the optode can be stored in a sealed bag either at room temperature or cold until use, with storage times measured in months with minimal changes to their sensitivity (Santner et al., 2015). Reference dyes are chosen depending on the indicator dye and generally emit light in different wavelengths to avoid overlapping with the emission from the indicator dye. The polymer depends on the desired analyte, since the analyte

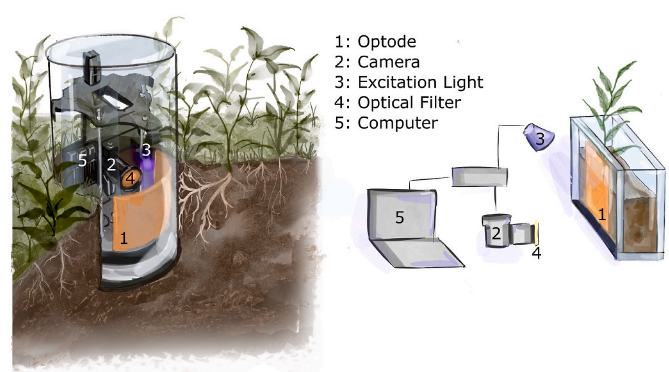

Fig. 1. Schematic overview of the general working principle of optodes and the required technical setup. Left: Drawing of the MARTINIS setup developed for in-situ imaging (Rasmussen et al., 2025) with the optode (1) in orange outside and the camera (2) and excitation light (3) source inside the transparent tube. Right: Sketch of a typical rhizobox setup, consisting of a glass container, soil with the investigated plant and an optode (1) in orange facing towards the inside. Both setups contain an optode (1), a camera (2), excitation light (3), and optical filters (4), together with the respective electronics to control acquisition (5). While both systems have a very different footprint, the essential components are the same. (For interpretation of the references to color in this figure legend, the reader is referred to the Web version of this article.)

needs to permeate through the polymer network to interact with the indicator dye for a change in the analytical signal. Polystyrene has a high gas permeability and is usually the preferred polymer for gaseous analytes. For ionic species, hydrogels with hydrophobic regions are used to allow access of the analytes to the more lipophilic indicator dye (Santner et al., 2015). Alternatively, poly (vinyl chloride) (PVC) with an appropriate plasticizer and ionophore can also be used. Additionally, fine particles (~2 μm) made of aluminum oxide, titanium oxide, or diamond powder can be added to the cocktail to increase homogeneity of the planar optode and the signal/noise ratio.

As mentioned above, planar optodes are imaged using a setup including a camera (Fig. 1) as the detector, an excitation light source, and an optional synchronizer (sometimes called trigger box) to coordinate the light source and the camera shutter. The light source excites the indicator dye in the optode while the camera records the intensity of the emission (or the lifetime change or the color change). It is important to note that when the sensor is based on luminescence intensity or color variations, the position, distance, and power of the light source need to be fixed for a repeatable and representative result. To perform the calibration for the correlation between signal change and analyte concentration, the optode is placed in a container with the sensor side facing inwards. The container is then filled with water to first determine the appropriate exposure and equilibration time for the optodes. Determining the correct exposure time prevents loss of data when too much light is entering the camera. Appropriate equilibration time is needed to allow the image to be taken at steady state of the interaction between the optode and the analyte. The calibration is then carried out by choosing five to eight concentration levels within the range of interest of the analyte and recording the corresponding emission or ratio. An in-depth discussion about calibration can be found in other articles and will not be further elaborated here (Rasmussen et al., 2026).

Optodes have been widely used in marine environments and sediments for more than three decades, whereas their application in soils emerged somewhat later (Glud et al., 1996; Blossfeld and Gansert, 2007; Askaer et al., 2010). Especially, the O_2 optode has advanced the understanding of biogeochemistry in marine water/sediment systems by characterizing the steep O_2 concentration gradient. Very similarly, DGT and DET (Diffusive equilibration in thin films) were used to obtain information about ion gradients. One reason why this transition into soil systems remained slow is that soils present a more complex physical environment for optode measurements. In waterlogged systems such as sediments, the sensor surface is typically in contact with a continuous water phase that allows relatively uniform diffusion of analytes to the sensing layer. In contrast, soils often contain both water- and air-filled pores, creating a heterogeneous transport environment. As ions (including protons) cannot diffuse through air-filled pores, the chemical conditions experienced by the optode may differ from those in the surrounding soil matrix. These features make optode deployment and interpretation more challenging in soils and partly explain why their broader adoption in terrestrial systems occurred later than in aquatic environments.

2.2. Methodological advantages of planar optodes

While point probes, such as microsensors or fiber-based sensors, are available for more analytes than the planar optode, the latter offers distinct advantages, such as the possibility of measuring two-dimensional maps within a single measurement. Point probes, however, need to be physically moved within the analyzed environment to achieve spatial measurements with a time delay between each point. Both point probes and planar optodes disturb the soil when introduced to the soil sample since they physically intrude into an undisturbed system. Planar optodes also introduce the so-called "wall effect" since the optode itself imposes a physical boundary on the sample and can alter local transport-reaction geometry (see section 5.2) (Polerecky et al., 2006). However, the information density obtained by the planar optode (which can reach the size of an A4 paper or larger) is much higher than that of a point probe. The resolution of the optode is mainly limited by the camera detector (pixel density) and optics used (lenses, optical pathways), allowing for the measurement of the analyte at the μm scale. Moreover, the maximum resolution further depends on the camera type, the picture format, and the chosen field of view. Santner et al. (2015) discussed this in greater detail in their review. Other advantages of planar optodes are their ability to be measured continuously and create a 2D distribution of the analyte over time (Koren and Zieger, 2021).

Aside from planar optodes, DGT and soil zymography have also been used to gain a 2D perspective into soil dynamics. DGT is based on the diffusion of an analyte through a gel into a captive layer, where the desired analyte is accumulated (Davison et al., 2007; Davison, 2016). Soil zymography follows similar strategies by trapping the products of the target enzyme in a membrane or providing substrates that are digested into fluorescent molecules (Bilyera and Kuzyakov, 2024). While DGT can be counted as a fully quantitative method, since all ions entering the gel are trapped, zymography does not bind its enzymatic products in a quantitative way and is thus a more qualitative method. However, both methods are irreversible, and the result represents an average over the time deployed in the soil. Planar optodes, on the other hand, are reversible and can be used for real-time determination of the analyte concentration for extended periods.

3. Optode applications in soil research

3.1. Oxygen: mapping of oxic/anoxic zones

Oxygen is one of the main "gatekeepers" of soil biogeochemistry. It sets the redox frame in which carbon mineralization proceeds (Keiluweit et al., 2016) and controls whether key element cycles run through aerobic pathways or switch to anaerobic transformations involving N, Fe, and S (Findlay et al., 2021). In particular, microscale O_2 gradients play a key role in the complex spatial variability of aerobic and anaerobic microbial respiration in soil, such as denitrification occurring within anoxic centers of mm-sized soil aggregates (Sexstone et al., 1985). These microscale redox interfaces can be quantified with the application of O_2 planar optodes that directly measure 2D spatial and temporal O_2 availability over cm^2-scale areas with a temporal resolution high enough to follow transitions and "hot moments" in redox state (Glud et al., 1996).

From a sensing perspective, O_2 optodes are among the most robust sensors in optical chemical sensing, relying on the reversible dynamic quenching of luminescent indicator dyes by O_2. Common indicator dyes include metal-ligand complexes Pt (II), Pd(II), Ir(III) porphyrins, and Ru (II) polypyridyl complexes, which combine high sensitivity with photostability (Wang and Wolfbeis, 2014). The O_2 optode response is traditionally described by variations of the Stern-Volmer equation (Schmidt-Böcking et al., 2016; Klimant et al., 1995) or by empirically fitted functions that better represent the full dynamic range (Rasmussen et al., 2026). These well-established methods for probing O_2 are a practical reason why O_2 is often the "entry point" for 2D chemical imaging in soils.

However, the luminescence response of O_2 optodes depends on temperature, which means that quantitative imaging requires temperature-aware calibration (or externally measured temperature) within the relevant range of the experiment, especially for long incubations or field deployments (Rickelt et al., 2013b; Rasmussen et al., 2025). In practice, this can be handled either by calibrating at multiple temperatures or by pairing O_2 imaging with temperature measurements (including temperature optodes) to support correction and interpretation (Koren and Kühl, 2015; Schwendt et al., 2024).

Although 2D sensing in soil science is still relatively young compared to sediment research, recent studies already illustrate why it matters. In upland soils at moderate moisture contents (~60% water-filled pore space, WFPS), O_2 optode imaging showed a partial decoupling between controls on bulk O_2 and the abundance of anoxic microenvironments (Keiluweit et al., 2018). A similar observation has been made from decomposition experiments in aerobic conditions (~50% WFPS), where localized microbial respiration induced anoxia and nitrous oxide (N_2O) production via denitrification (Lussich et al., 2024), despite the classical expectation that O_2 limitation (and thus denitrification) becomes dominant only at higher WFPS (≥70%) (Bateman and Baggs, 2005; Wang et al., 2023). Together, these results highlight the importance of measuring O_2 directly at the spatial scales to estimate microbial activity, rather than assuming that bulk O_2 or WFPS alone can predict greenhouse gas (GHG) formation or carbon mineralization (Keiluweit et al., 2017; Song et al., 2019; Lacroix et al., 2023).

Optode imaging has thus been used to visualize how organic amendments and fertilizer practices shape spatiotemporal oxygen distributions, and how these redox patterns relate to soil emission and nutrient turnover. Examples include studies on organic manure distribution and incorporation (Zhu et al., 2014), manure application combined with nitrification inhibitors (Nguyen et al., 2017), and localized incorporation of straw or biochar patches that create strong local shifts in oxygen availability (Zhu et al., 2014). These applications highlight the use of 2D oxygen mapping to reveal mechanistic links for potential anaerobic microbial respiration in otherwise bulk oxygenated soil.

Finally, oxygen imaging is particularly powerful in systems where soil biology actively reshapes redox structure. In waterlogged soils, optodes have been widely used to quantify rhizosphere oxygen dynamics and radial oxygen loss from roots (Koop-Jakobsen and Wenzhöfer, 2015; Larsen et al., 2015), linking root physiology to microbial habitat structure and redox-driven reactions at the root/soil interface (Blossfeld et al., 2011; Lenzewski et al., 2018). In non-waterlogged soils, macrofauna can also cause equally drastic redox restructuring: dung beetle activity, for example, redistributes organic matter and generates pronounced anoxic zones (Natta et al., 2025) (Fig. 2).

Looking forward, the main near-term value of O_2 optodes in soils is to make mechanistic experiments more diagnostic and more comparable across systems. Continued progress will likely come from tighter integration of O_2 maps with complementary measurements (e.g., gas fluxes, microsensors, targeted microsite sampling; see Section 4) to better understand the physiology and environmental impact of plants, fauna, and microbial activity in soils. To support this progress, implementation of calibration practices that enable quantitative cross-study interpretation are highly needed (Rasmussen et al., 2026).

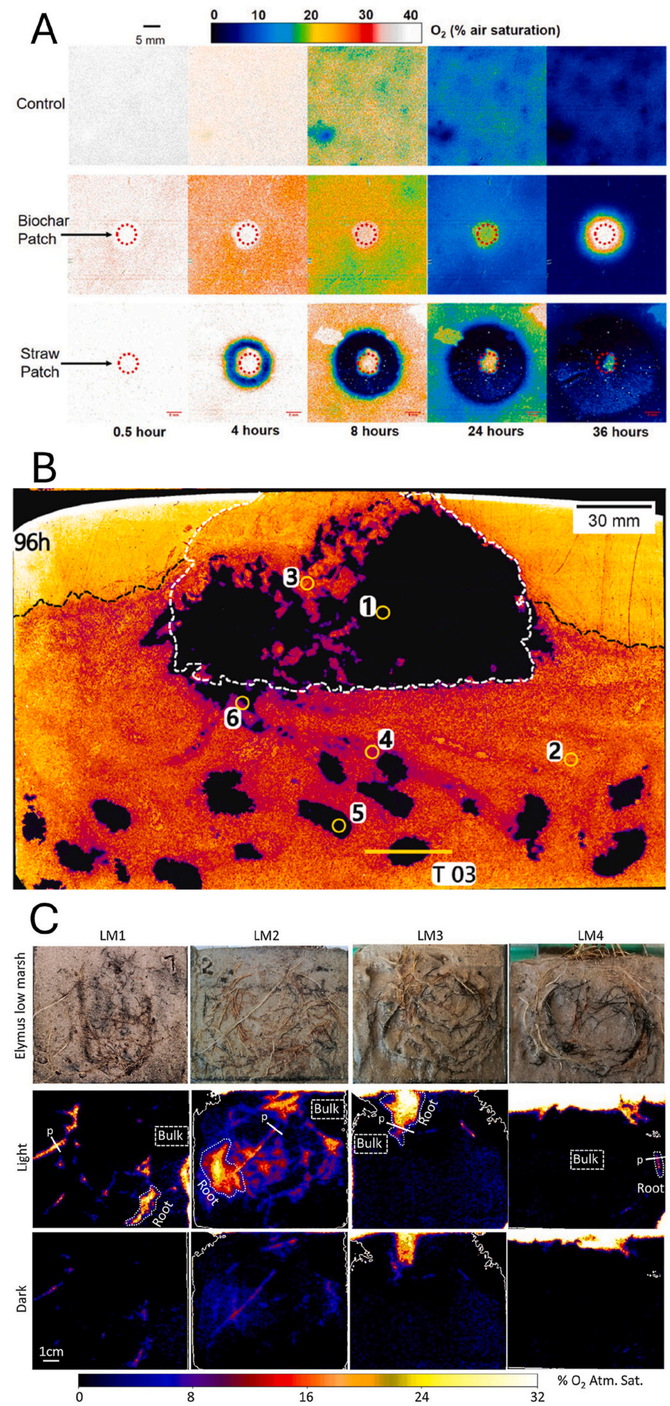

Fig. 2. Examples of using O_2 optodes in soil research. A: Spatial oxygen heterogeneity generated by organic matter hotspots (e.g., straw, manure, biochar), creating localized zones of rapid O_2 depletion in soil (Zhu et al., 2022). B: Soil oxygen heterogeneity generated by dung beetle activity, forming oxic and anoxic microsites through bioturbation and organic matter redistribution (Natta et al., 2025). C: Rhizosphere oxygen heterogeneity generated by root activity, forming localized oxic zones and steep O_2 gradients between root surfaces and surrounding bulk soil (Koop-Jakobsen et al., 2021).

3.2. Carbon dioxide: respiration patterns and C-cycling hotspot

CO_2 is a key analyte as it is the product of plant and microbial respiration processes in soil. Planar optodes for CO_2 are often based on fluorescent pH-sensitive indicators (Ind) combined with a lipophilic base (often a tertiary amine like tetraoctylammonium, TOA) and subsequently embedded in a polymer support (often ethyl cellulose), the so-called Mills type sensor (Mills and Chang, 1993; Schutting et al., 2014). The acidic gas CO_2 can diffuse into the sensor and react with the base, forming an ion pair and protonating the indicator (Eq (2)).

$$Ind^{-}TOA^{+} + CO_2 + H_2O \leftrightarrow IndH + TOA^{+}HCO_3^{-} \quad (2)$$

This protonation of the indicator dye leads to a change in either the emission spectra or intensity of the indicator, which can be detected and related to the CO_2 concentration via calibration. Obviously, this approach makes the sensor vulnerable to other acid gases that can react with the indicator base pair, such as H_2S. Furthermore, this sensing principle requires water within the sensing layer to facilitate the acid-base reaction, limiting it to moist and wet soil conditions. Long-term stability of CO_2 optodes is inferior compared to O_2 optodes, for example (Table 1).

With respect to soil imaging with CO_2 optodes, there exist only a handful of examples. CO_2 optodes were applied to visualize root respiration of *Viminaria juncea* (Blossfeld et al., 2013), *Spartina anglica* (Koop-Jakobsen et al., 2018), *Lupinus albus* (Bereswill et al., 2024) (Fig. 3), and *Zea mays* (Holz et al., 2020). Under dry conditions, elevated CO_2 levels were only detected in the direct vicinity of roots (Holz et al.,

Table 1
Overview of analytes measurable with planar optodes and typical characteristics.

Analyte	Working range	Response time	Imaging modes[a]	Key caveats/Cross-sensitivities[b]	Adoption in soil research	References
O_2	0–210 (up to 1000) hPa pO_2 (0–100% (up to 500%) air saturation)	Seconds–tens of seconds (foil-dependent)	CR; WR, lifetime (RLD, t-DLR)	Contact loss in dry soils; illumination gradients	Routine in soils; commercial foils & imaging systems exist	(Blossfeld et al., 2011; Koop-Jakobsen and Wenzhöfer, 2015; Wolfbeis, 2015; Rummel et al., 2026)
pH (H^+)	pH 5–9 typically narrow (≈pKa ± 1–1.5)	~5 min or faster (setup-dependent)	CR; WR, t-DLR	Requires hydration; ionic strength sensitivity for some dyes; range-limited	Common in soils; commercial foils; chemistry must match the pH range of the soil	(Rudolph et al., 2013; Buss et al., 2018; Merl and Koren, 2020)
CO_2/pCO_2	0–41 hPa pCO_2 (0–40 matm)	Several minutes	WR or FD (design-dependent)	H_2S interference in some designs; slow equilibration in soils	Strong in sediments; emerging in soils; some commercial systems	(Blossfeld et al., 2013; Koop-Jakobsen et al., 2018; Lenzewski et al., 2018; Bereswill et al., 2024)
NH_3 (gas)	0–1.82 hPa pNH_3 (0–1800 ppm)	Minutes-scale; configuration-dependent	Color/WR intensity imaging	Headspace & humidity effects; drift; open-system losses	Emerging in soils; requires careful calibration and validation	(Strömberg and Hakonen, 2011; Merl and Koren, 2020; Merl et al., 2023)
NH_4^+	10 µmol L^{-1}–100 mmol L^{-1}	Several minutes (system-dependent)	CR, WR	K^+ and ionic strength interference; calibration matrix dependence	Demonstrated in soils/rhizosphere; niche use	(Strömberg, 2008; Delin and Strömberg, 2011)
NO_3^-	1–50 mmol L^{-1}	Seconds–minutes	Intensity, CR	Strong NO_2^-, Cl^-, SCN^- interference	Proof-of-concept; not shown in soils research	Pedersen et al. (2015)
Temperature	0–60 °C	Several seconds	CR, Lifetime (RLD)	Often used to correct/support other analytes	Useful companion layer; some commercial options	(Rickelt et al., 2013a; Rasmussen et al., 2025)

[a] Abbrev.: CR = color ratiometric (intensity-based); WR = wavelength ratiometric (intensity-based); RLD/t-DLR/FD = lifetime-based approaches (rapid lifetime determination, time-domain luminescence ratio, frequency domain).
[b] All optodes are temperature cross-sensitive.

2020), while elevated CO_2 levels reach millimeters away from the root in wet and waterlogged conditions (Blossfeld et al., 2013; Koop-Jakobsen et al., 2018; Bereswill et al., 2024). Combining CO_2 and O_2 optodes, O_2 release and CO_2 uptake from roots were observed from *Lobelia dortmanna* during photosynthesis, resulting in a CO_2 depletion around the roots and a zone of increased respiration further away from the roots (Lenzewski et al., 2018) (Fig. 3). Despite its key role in soils, studies visualizing CO_2 dynamics with optodes are scarce. Lack of stability and more difficult calibration procedures limit their applicability. Nevertheless, even qualitative imaging can be very useful to identify hotspots that could be further analyzed with destructive sampling.

3.3. pH: rhizosphere and decomposition chemistry

Measurement of pH involves the exchange of protons between water in the soil and the fluorescent pH indicator (Ind, Eq (3)). Protonated and deprotonated indicator dyes usually have different emission intensity or spectra, providing the analytical signal. The measurable pH range can be estimated by adding and subtracting 1.5 pH units from the pK_a value of the indicator dye. The pK_a is formally defined as the negative logarithm of the acid dissociation constant of the indicator-water pair. It denotes the pH at which both protonated and deprotonated forms of the indicator dye are present at equal concentration and therefore marks the point at which the greatest change in the analytical signal occurs.

$$Ind^- + H_3O^+ \leftrightarrow IndH + H_2O \qquad (3)$$

Changes in pH within a soil sample can be related to various influences, such as bacterial community composition, erosion history, mineralogy or changes thereof, and release of gases such as nitrous acid (HONO), ammonia (NH_3), or nitrous oxide (N_2O) (Kim and Or, 2019; Merl et al., 2022). Particularly changes with diurnal patterns, near rhizospheres or at decomposition sites, are interesting as they offer insights into soil fertility, biogeochemical cycling, and bioprocesses of roots. For example, diurnal pH changes are closely linked to CO_2 cycles and soil respiration (Harper et al., 1983; Dawson et al., 2001; Nishimura et al., 2015; Russenes et al., 2016). In the rhizosphere, pH variations are linked to the uptake of nutrients through the root system. The roots release H^+ ions to establish a positive electropotential between the cytosol and the rhizosphere, which provides the necessary energy for the co-transport of the H^+-anion pair and for cation uptake via H^+ release. Depending on the anion/cation uptake balance, the H^+ uptake or release can lead to an overall pH increase or decrease in the rhizosphere, respectively (El-Shatnawi and Makhadmeh, 2001; Neumann and Römheld, 2012; Dotaniya and Meena, 2015). Moreover, the consequences of soil acidification or neutralization on the microbial community, as well as their adaptation to the pH change, can also be studied (Bååth, 1996; Fierer and Jackson, 2006; Bartram et al., 2014). Fertilization is another aspect where soil pH plays an important role as common N fertilizer sources include ammonium, urea and nitrate, which induce changes in soil pH upon addition and subsequent nitrification or denitrification reactions (Recous et al., 1992; Kissel et al., 2008; Rochette et al., 2013; Wang et al., 2020).

Soil pH also reflects its use or recent major events that happened. For example, regularly fertilized soil used as agricultural land may have lower pH values than non-fertilized soil, which underlines the importance of the application of lime or other acid-neutralizing materials to maintain neutral pH values (Goulding, 2016). When a major event, such as wildfire, influences the soil sample, the pH change is visible for a long time. Immediately after the fire, soil pH increases drastically over 2 to 3 units and is buffered by the soil itself on the first day after the fire (Honeyman et al., 2023). This increase is due to the formation of alkaline carbonates and metal oxides. Ashes from the vegetation continue to keep a high pH until leaching, erosion, and the formation of a new humus layer removes the excess of these basic (cat)ions, a process which can vary between a few months to several years (Gómez-Rey et al., 2013; Muñoz-Rojas et al., 2016; Fernández-García et al., 2019).

Planar optodes for pH measurements have been successfully used to understand processes in the rhizosphere (Blossfeld and Gansert, 2012; Blossfeld et al., 2013), after applying manure (Merl and Koren, 2020) (Fig. 4), and visualizing soil fauna contribution to fertilizer distribution (Natta et al., 2025). Additionally, interfaces between soil and other substances can be visualized (Buss et al., 2018), and seasonal changes in marine sediment studied (Fan et al., 2011; Han et al., 2016).

3.4. Ammonia: emission hotspots and mitigation

Ammonia (NH_3) gas emissions from soil processes impact not only the soil itself but also the formation of atmospheric particulate matter. Agriculture and, particularly, fertilizer and manure management are the largest sources of NH_3 in the atmosphere globally (Behera et al., 2013).

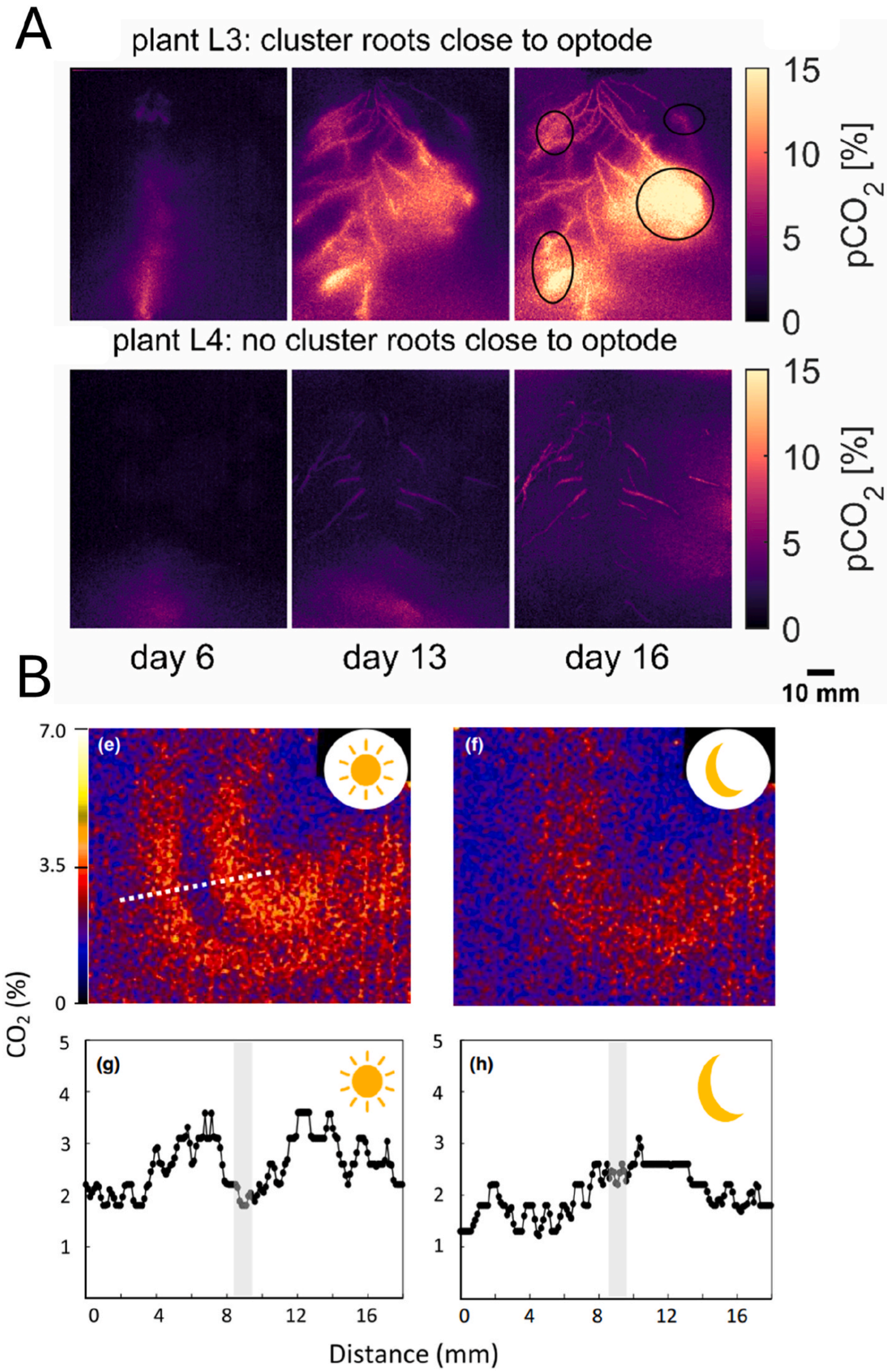

Fig. 3. Examples of CO_2 optodes in soil research. A: CO_2 distribution in soil showing localized CO_2 enrichment linked to microbial respiration and soil structure heterogeneity (Bereswill et al., 2024). B: Diurnal variation of soil CO_2 concentration measured by planar optodes, illustrating higher CO_2 levels during daytime and lower levels at night due to root and microbial respiration dynamics (Lenzewski et al., 2018).

This has led to the development of several methods to measure NH_3 fluxes into the atmosphere (Scotto di Perta et al., 2020). While it is evident that NH_3 emission is a large-scale problem, the process that leads to the volatilization is found at the microscale (Sommer et al., 2003). Ammonia exists in a pH-dependent equilibrium with ammonium (NH_4^+). The pK_a of this system is approximately 9.2, depending on temperature. Consequently, at acidic and neutral pH, the fraction of free NH_3 is negligible, and NH_4^+ dominates.

Ammonia optodes have been around for decades with a clear focus on detecting very low (ppb) levels of dissolved NH_3 in aquatic systems (Waich et al., 2007; Abel et al., 2012; Strobl et al., 2017). The reasoning behind this focus is that NH_3 is toxic to aquatic organisms even at those low concentrations (Randall and Tsui, 2002). From a soil standpoint and with respect to NH_3 volatilizations, much higher (up to 200 ppm) levels can be expected (Timmer et al., 2005). With this in mind, Merl and Koren developed the first dedicated NH_3 optode for soil studies (Merl and Koren, 2020).

Similar to the CO_2 sensor, the NH_3 sensor is based on a gas-permeable membrane to prevent ionic species from entering the sensor. Behind this membrane, a pH-sensitive dye (Oxazine 170) is immobilized in a hydrogel matrix together with a reference dye. Upon deprotonation, NH_3 acting as the base in this case, Oxazine 170 changes

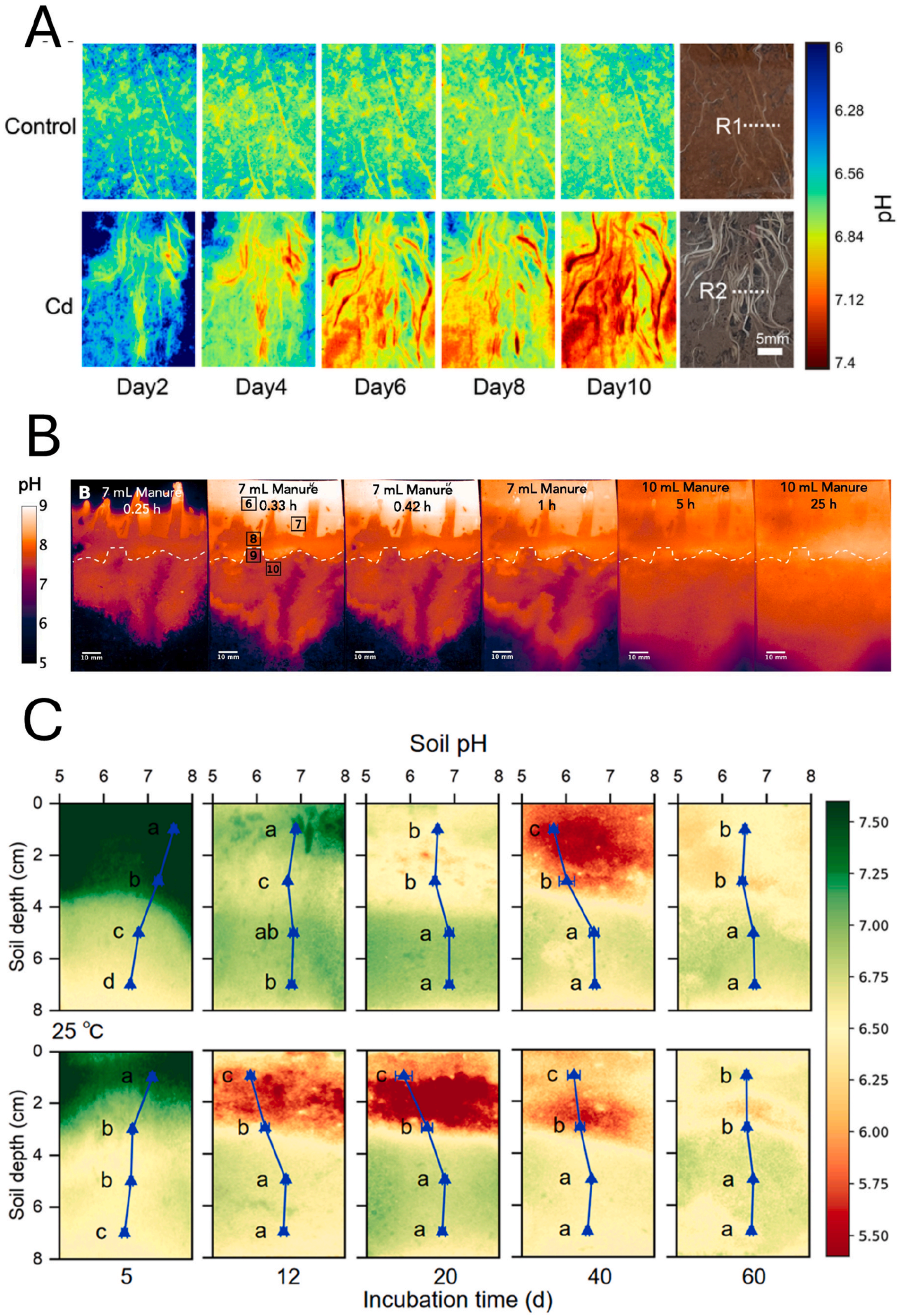

Fig. 4. Examples of using pH optodes in soil research. A: Rhizosphere pH heterogeneity in the control and Cd-treated *Celosia argentea* (Ge et al., 2025). B: Soil pH heterogeneity generated by organic amendment (manure) (Merl and Koren, 2020). C: Localized soil acidification generated by microbial nitrification following urea fertilization, producing distinct pH gradients in the soil profile over time (Tao et al., 2025).

its emission characteristics (Eq. (4)). This can be detected using an RGB camera and, upon calibration, translated into a local NH_3 concentration.

$$NH_3 + IndH^+ + Ref \leftrightarrow NH_4^+ + Ind + Ref \quad (4)$$

In the first soil study, NH_3 volatilization after addition of manure was visualized in combination with pH and O_2 optodes (Merl and Koren, 2020) (Fig. 5). Intense peaks directly after the manure application were observed. This can largely be explained by the free NH_3 within the manure being volatilized as the surface increases enabling a better gas exchange. Following this, the NH_3 optode was further evaluated and tested with respect to the placement of the fertilizer on the soil surface compared to deep in the soil. The optode revealed that placing the fertilizer, in this case dairy processing sludge, in the soil reduced the emission of NH_3 significantly (up to 87% compared to surface application) (Merl et al., 2023). Furthermore, this study showed that NH_3 optodes are cross-sensitive to humidity and, as such, require a simultaneous humidity measurement to get quantitative data. Correcting this cross-sensitivity is possible, but often even uncorrected qualitative information can be helpful to locate hotspots of NH_3 emission (Hu et al., 2024). Such hotspots were observed in the surroundings of mineral fertilizers; it was possible to combine pH and NH_3 optodes to track those parameters in the "fertosphere" (Lombi et al., 2025) over an extended period (up to 65 h) (Merl et al., 2024) (Fig. 6). The chemical images obtained by the optodes then informed localized sampling for both chemical (different nitrogen species) and molecular (transcription) analysis showcasing how chemical imaging with optodes can be used to inform other types of analysis and can be a "chemical GPS" in complex environments like soils.

Ammonia optodes are still new to soil analysis but have already shown promising results. One of the positive aspects of this optode is the commercial availability of all the materials needed. While preparing the membrane-covered optode requires some practice, this makes them accessible and easily integrable.

3.5. Ionic species

Ion-selective optodes have been developed for several important ions in agriculture and biogeochemistry, including ammonium (NH_4^+), potassium (K^+), and nitrate (NO_3^-). However, their application in intact soils remains very limited compared to planar optodes designed for gases and pH measurement. This limitation arises from fundamental challenges related to membrane stability and ion selectivity, including the inherent pH cross-sensitivity of conventional ion-selective optodes. Additionally, strong matrix effects, caused by heterogeneous soil porewater environments, variable moisture conditions, and fluctuating ionic strength, further restrict the widespread use of ion-selective optodes.

Among these ions, NH_4^+ has received the most attention at the application level, including several pioneering demonstrations in soil and rhizosphere systems. Early optode designs based on the ionophore nonactin used as a selective complexation agent demonstrated strong cross-sensitivity between NH_4^+ and K^+ due to their similar ionic radii and hydration energies (Seiler et al., 1989). Despite this limitation, planar ammonium optodes were successfully adapted for soil-relevant applications. Strömberg et al. demonstrated imaging of ammonium turnover close to intact tomato roots using planar optodes, resolving depletion zones, uptake heterogeneity along root structures, and temporal dynamics over diel cycles (Strömberg, 2008; Delin and Strömberg, 2011). However, ammonium optode measurements require careful control of ionic strength, pH, and interfering ions, and typically rely on sophisticated calibration schemes to compensate for signal drift and short-term stability.

Optode-based sensing of NO_3^- and K^+ faces similar, if not greater, limitations. Nitrate-selective (Pedersen et al., 2015) and valinomycin-based K^+-selective optodes (Kassal et al., 2019) have been demonstrated in aqueous systems, but typically suffer from pronounced interference by NH_4^+, NO_2^- (nitrite), and other oxyanions, severely limiting their applicability in chemically complex soil environments (Damala et al., 2023). Consequently, NO_3^- and K^+ measurements in soils continue to rely on extraction-based analyses, DGT techniques, or electrochemical sensors rather than optical imaging approaches (Ameer et al., 2024).

Overall, ion-selective optodes are a promising but underutilized frontier in the field of soil chemical imaging. Their limited use in soil research is mainly due to ongoing challenges related to ion interference and the difficulty of achieving reliable calibration in varied porewater environments. Future advancements will depend on significant improvements in membrane chemistry, strategies to suppress interference, and the development of calibration methods, which are specific to soil applications. Only then can ion-selective optodes have a meaningful impact on spatially resolved soil biogeochemistry.

4. Linking co-occurring chemical processes in soils — multiparameter imaging

One of the central advantages of planar optode approaches is their ability to support multianalyte imaging, enabling simultaneous observation of multiple chemical parameters within the same soil system. Because soil biogeochemical processes are inherently coupled, multiparameter measurements provide a more holistic representation of soil microenvironments and allow mechanistic interpretation of spatial and temporal co-occurrence patterns. In contrast to single-analyte imaging, which may capture only one facet of a process, multianalyte optode approaches reveal how gradients in O_2, pH, NH_3, and CO_2 interact to shape biogeochemical hotspots.

4.1. Multiparameter optode strategies and technical implementations

Multiparameter optode imaging generally follows two conceptual strategies. In the first, multiple indicator dyes are incorporated into a single sensing layer or stacked multilayer films, and individual analytes are resolved through separate optical channels or spectral unmixing. In the second, distinct optode foils, or optodes combined with complementary planar techniques such as DGT, are co-deployed within a shared experimental geometry. The principles, limitations, and analytical considerations underlying these approaches have been comprehensively reviewed elsewhere (Kalinichev et al., 2023).

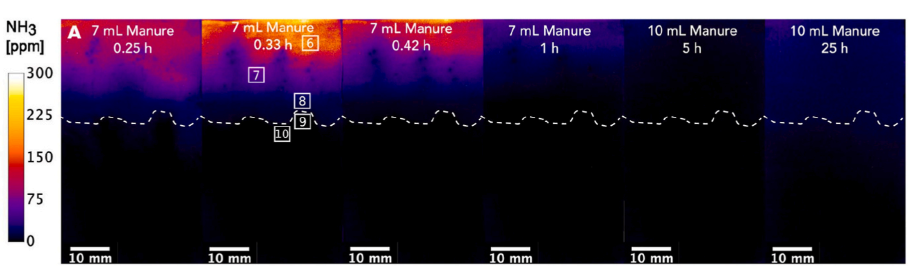

Fig. 5. Example of using NH_3 optodes in soil research. Distribution of gaseous NH_3 levels above soil, following manure application at different time points, demonstrating the rapid temporal dynamics at the soil/air interface (Merl and Koren, 2020).

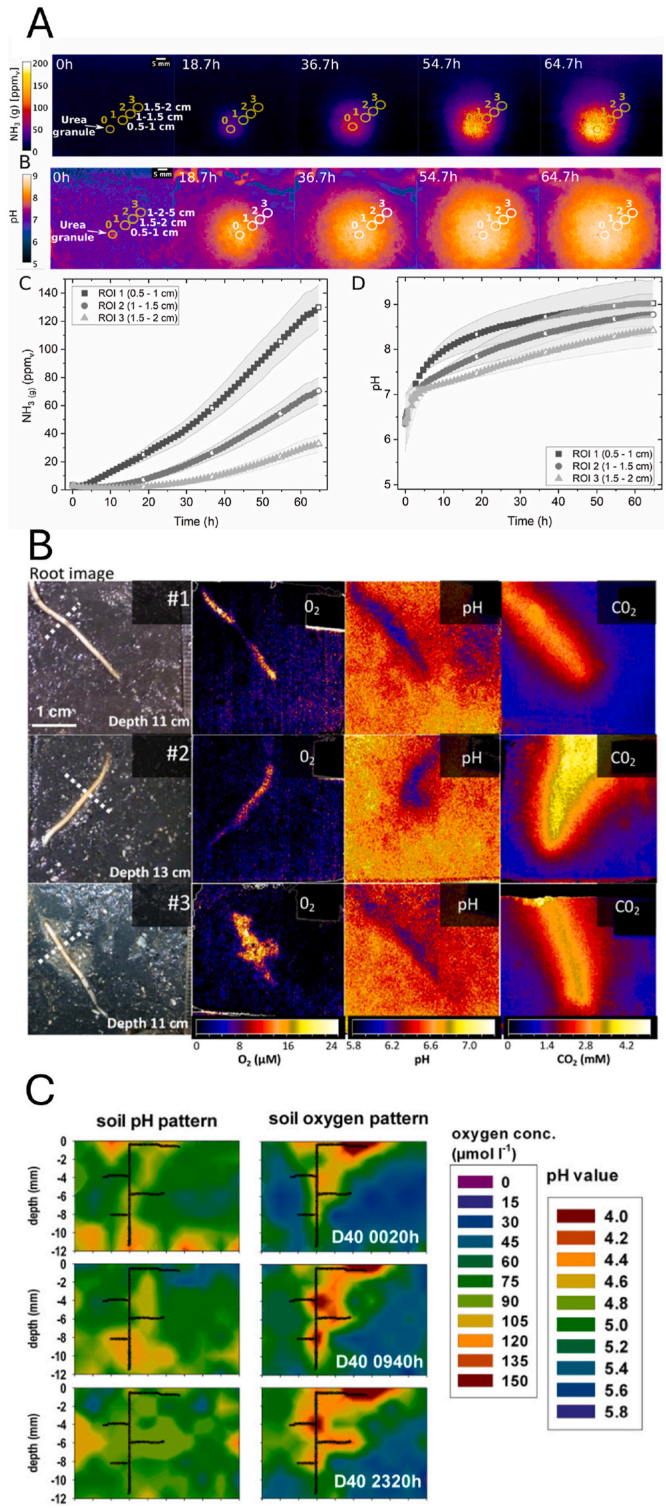

Fig. 6. Examples of multiparameter mapping of soil using planar optodes. A: Combined imaging of NH_3 and pH dynamics in soil surrounding a urea granule, illustrating the spatial coupling between ammonia formation and alkalization during fertilizer hydrolysis (Merl et al., 2024). B: Simultaneous mapping of O_2, pH, and CO_2 around roots in the rhizosphere, revealing strong spatial gradients driven by root activity and microbial respiration (Koop-Jakobsen et al., 2018). C: Time-series imaging of pH and O_2 distributions around lateral roots, demonstrating dynamic changes in rhizosphere chemistry over time (Blossfeld et al., 2011).

The majority of state-of-the-art approaches are still focused on dual-parameter imaging, reflecting a practical compromise between experimental complexity and interpretability. Technically, dual imaging has been implemented using camera systems equipped with multiple emission filters or channels (Moβhammer et al., 2016), phase- or frequency-resolved detection for lifetime-based sensing (Borisov et al., 2006), hyperspectral imaging that enables spectral separation of overlapping dyes (Bognár et al., 2024; Schwendt et al., 2024), or spatially distributed grid optodes in which different sensing chemistries are patterned across defined regions of a single substrate (Kalinichev et al., 2025). These approaches have enabled robust acquisition of paired chemical maps at mm-to µm-resolution, suitable for capturing soil microscale heterogeneity.

4.2. *Oxygen, pH, and CO_2: coupled redox and acid–base dynamics*

Among the most established combinations in soil research are O_2 and pH, highlighting their central roles in redox regulation and acid–base buffering. Dual O_2/pH optodes, in which an O_2-sensitive luminophore and a pH-sensitive dye are co-embedded within the same film, allow direct visualization of oxic–anoxic transitions alongside associated H^+ dynamics. Alternatively, O_2 and pH optodes have been deployed in parallel to examine spatial correlations in the rhizosphere and organic matter hotspots. Early rhizosphere studies demonstrated that O_2 depletion due to root respiration and pH modification through H^+ fluxes are often spatially coupled but not necessarily co-localized, with oxidized, high-pH zones near certain root segments and adjacent anoxic, more acidic microsites further away (Blossfeld et al., 2011; Koop-Jakobsen et al., 2018).

More recent work has extended combined O_2 and pH imaging to structurally complex soil–fauna systems. In a dung beetle experiment, concurrent O_2 and pH mapping revealed sharp chemical contrasts between beetle tunnels and dung-rich microsites, with pronounced redox gradients and pH shifts across mm-scales (Natta et al., 2025). These multiparameter observations were essential for mechanistically linking bioturbation-induced changes in soil structure to enhanced oxic/anoxic interface area.

Integration of pH and CO_2 sensing further enriches mechanistic interpretation by directly linking respiration-driven CO_2 production to acid–base dynamics. An integrated pH/CO_2 planar sensor has been applied in rhizosphere studies to show that localized pH decreases coincide with CO_2 accumulation arising from root and microbial respiration (Blossfeld et al., 2013). Such observations help disentangle whether pH shifts are primarily driven by biological CO_2 production, carbonate buffering reactions, or nutrient uptake processes, which are often difficult to separate using bulk measurements.

4.3. *Ammonia, pH, and oxygen: investigation of nitrogen hotspots*

Multiparameter imaging has proven particularly informative for investigating ammonia dynamics, where NH_3 availability, pH, and O_2 status are tightly interlinked. Recent ammonia optode studies employed coordinated combinations of NH_3, pH, and O_2 optodes within the same soil sandwich framework to investigate NH_3 hotspots under contrasting moisture and aeration regimes (Merl and Koren, 2020; Merl et al., 2023, 2024). By integrating multiple parameters across experiments, these studies demonstrated that NH_3 emission, microsite alkalization, and O_2 availability cannot be interpreted independently. For instance, under dry, well-aerated conditions, rapid NH_3 release coincided with strong local pH elevation, whereas under wetter, O_2-limited conditions, NH_3 diffusion was slower.

4.4. *Integration of optodes with tracers and complementary planar techniques*

Beyond combinations of different optodes, chemical imaging has been successfully integrated with physical tracers and complementary analytical techniques. In the dung beetle study, fluorescent tracers were incorporated into dung to visualize its physical redistribution under fully anoxic conditions, where oxygen optodes alone provided no contrast. Combining tracer-based visualization with optode-derived chemical maps enabled spatial alignment of organic matter placement with persistent anoxic zones, strengthening causal interpretation of observed biogeochemical patterns (Natta et al., 2025).

Furthermore, co-deployment of planar optodes with DGT has enabled spatially resolved linkage between soil chemical conditions and nutrient availability. While optodes provide two-dimensional, time-resolved maps of parameters such as pH or O_2, DGT gels integrate solute fluxes over time and thus reflect the labile nutrient pool accessible for diffusion and uptake. Combining these approaches allows direct assessment of how microscale chemical gradients regulate nutrient mobilization in heterogeneous soils. In a biochar-amended soil, Chen et al. used a pH optode in conjunction with a phosphate-binding DGT layer to demonstrate that localized pH increases around biochar particles coincided with enhanced phosphorus fluxes, revealing strong mm-scale heterogeneity not captured by bulk measurements (Chen et al., 2024). Similar optode-DGT configurations have been applied to rhizosphere systems, where root-induced pH gradients were shown to exert strong control over the spatial distribution of labile phosphorus and micronutrients (Bornø et al., 2023). More generally, combined chemical imaging and DGT approaches provide a mechanistic framework for identifying microsites where soil chemistry promotes nutrient mobilization or immobilization (Lehto et al., 2017). Although optodes and DGT operate on different temporal principles (instantaneous vs time-integrated), their co-deployment enables complementary insight into the coupling between soil chemical dynamics and nutrient supply at the microscale (Fig. 7).

4.5. Multimodal integration

An emerging form of multimodal integration involves using optode maps to guide targeted biological or geochemical sampling. Honeyman et al. introduced the concept of a "chemical navigator" (Fig. 7) in which O_2 and pH optode images were used to inform spatially resolved RNA sampling in fire-affected soils, enabling direct correlation between chemical microenvironments and gene expression patterns (Honeyman et al., 2023) (Fig. 8). Such approaches highlight how planar optodes can function not only as diagnostic tools but also as strategic frameworks for integrating chemical imaging with molecular and mineralogical analyses.

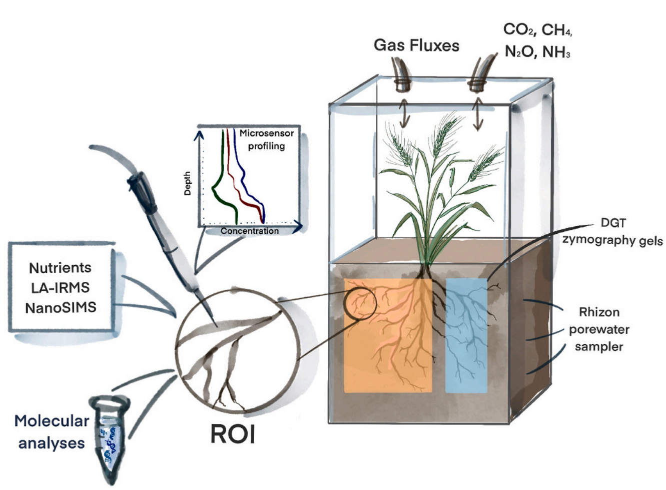

Fig. 7. Conceptual figure illustrating how optodes (in orange) can be combined with complementary techniques and how they can guide the finding of regions of interest (ROI) in complex systems. Those ROIs can then be further analyzed with other nondestructive or destructive measurements. (For interpretation of the references to color in this figure legend, the reader is referred to the Web version of this article.)

A similar "chemical GPS" logic was used in a recently published rhizobox study, where planar O_2 optode imaging and root imaging were not only used to visualize heterogeneity, but to define regions of interest for additional measurements (Rummel et al., 2026) (Fig. 8). Based on root presence/age and local redox state (e.g., anoxic patches at the optode/soil interface), these regions were subsequently targeted for complementary, higher-specificity measurements that cannot be obtained from optodes alone: direct *in-situ* N_2O concentration profiles with Clark-type N_2O microsensors, microsite nutrient status (NO_3^-, NH_4^+, DOC), and functional gene abundances (nirK/nirS and nosZ clades) from small-volume soil sampling. This workflow reduced "blind" sampling and enabled mechanistic links between O_2 microenvironments, substrate availability, microbial function, and the emergence of N_2O hotspots in the rhizosphere, guided by the obtained O_2 maps.

Another promising direction for multimodal integration is the combination of planar optode imaging with three-dimensional structural characterization, particularly X-ray micro-computed tomography (μCT). While μCT cannot directly quantify chemical species such as O_2, pH, or nutrients, it provides high-resolution information on soil pore architecture, air- and water-filled porosity, and aggregate structure, all of which strongly control gas diffusion and microbial habitat connectivity. A concrete example of such integration was provided by Keiluweit et al. who combined planar O_2 optode imaging with μCT characterization of the same upland soils (Keiluweit et al., 2018). By jointly interpreting these datasets, they demonstrated that the persistence of anoxic microsites was not governed by bulk O_2 availability but by diffusion limitations imposed by clay-rich, poorly connected pore networks. In addition, Rohe et al. demonstrated that μCT-derived metrics of air connectivity and diffusion distance can be used to estimate anaerobic soil volume fractions as structural proxies for O_2 supply, especially when interpreted together with O_2 demand (e.g., respiration) (Rohe et al., 2021).

Together, these studies motivate future workflows that more tightly couple (and ideally co-register) 2D optode maps with μCT-derived pore networks to resolve the physical drivers of soil biogeochemical hotspots across scales.

4.6. Future directions

Overall, multianalyte planar optode imaging provides uniquely powerful insights into soil biogeochemical coupling. By capturing interacting gradients of the combination of key soil parameters, these approaches move soil research closer to a system-level understanding of microscale heterogeneity. By capturing more than one parameter, planar sensors can directly show cause-and-effect relationships: e.g., an optode image might show pH drops exactly where O_2 is low, confirming acidification is linked to anaerobic respiration. This type of insight moves us closer to a 2D process visualization. As new dyes and methods continue to advance (for NO_3^-, redox potential, enzyme activity, etc.), multiparameter optode systems are likely to become in situ "micro laboratories" for studying the complex biogeochemistry of soil microsites in real time.

5. Critical perspective: what optodes can and cannot tell us

In 1966, Abraham Maslow wrote, "… it is tempting, if the only tool you have is a hammer, to treat everything as if it were a nail." (Maslow, 1966) Optodes are one of the authors' favorite tools. That is not a problem, until we start using them as the default answer to every question. This section is about finding the *right nails* (problems) for the *optode hammer* (as a method): when are optodes helpful, when are they not, and how can they be combined with other methods to address mechanistic questions in soil biogeochemistry?

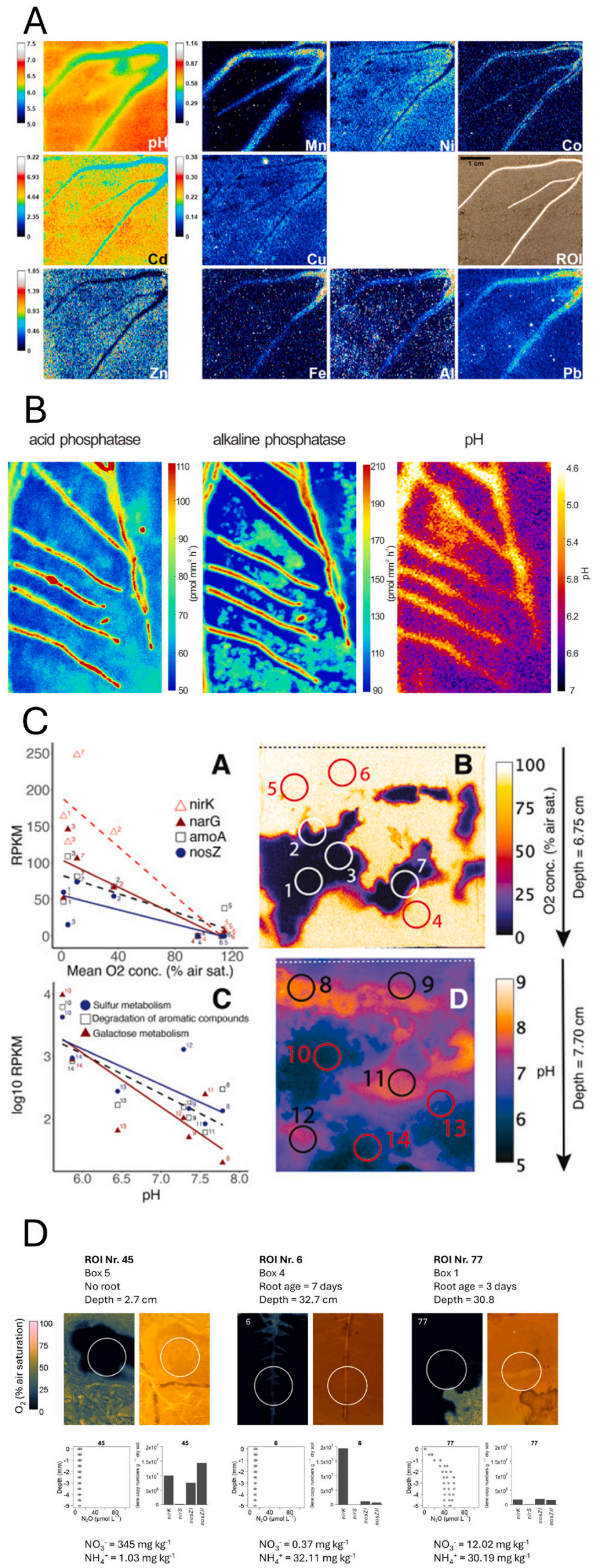

(caption on next column)

Fig. 8. Examples of multimodal approaches combining optode imaging with complementary techniques. A: Integration of planar optode imaging with DGT measurements to relate spatial patterns of pH with the distribution and fluxes of dissolved metals in the rhizosphere (Hoefer et al., 2017). B: Combined mapping of enzyme activities (acid and alkaline phosphatase) together with pH around plant roots, highlighting how biochemical processes and chemical gradients co-occur in the rhizosphere (Ma et al., 2021). C: Use of O_2 and pH optode maps to guide spatially resolved biological sampling and link soil chemical micro-environments with gene expression patterns (Honeyman et al., 2023). D: Application of O_2 optode imaging as a "chemical navigator" to identify microsites for targeted measurements of nitrogen transformations and associated microbial processes (Rummel et al., 2026).

5.1. What optodes can do well: showcase heterogeneity and reveal dynamics

The core strength of planar optodes is that they turn a bulk average into a spatially resolved story. A soil can appear "well oxygenated" by bulk measurements and still contain anoxic microsites that sustain fundamentally different metabolisms and reaction pathways. Optodes make such microsites visible, and they can do so continuously over time, enabling a dynamic perspective that is hard to obtain with other methods. This spatiotemporal capability is especially powerful for mechanistic investigations: optodes can reveal co-occurrence patterns (e.g., O_2 depletion co-localizing with pH shifts or CO_2 accumulation), identify hotspots and boundaries (oxic/anoxic interfaces, rhizosphere gradients), and generate hypotheses about controls and feedbacks occurring in soils. In multiparameter configurations, optodes also provide the kind of coupled observations that are needed to move just from "maps" to "process narratives." For example, it can help distinguish whether a pH change is associated with respiration-driven CO_2 accumulation, nitrification-driven acidification, or alkalization linked to NH_3 generation. In this sense, optodes are not only visualization tools; they can provide information for further microsite-aware modeling.

A second practical strength is that optodes are largely (every measurement technique alters the sample even if only slightly) non-destructive and can be used over extended periods (days to weeks, sometimes longer depending on the sensor chemistry and conditions). That makes them ideal for experiments where disturbance would erase the very heterogeneity of interest, such as rhizosphere development, bioturbation, wetting-drying transitions, or amendment-induced hotspot formation. Compared to endpoint sampling or time-integrating methods (e.g., DGT, zymography), optodes provide a continuous "movie" of chemical microenvironments.

5.2. What optodes cannot do (yet): fluxes, 3D imaging, and calibration-free modes

At the same time, optodes have limits that must be built into the experimental logic. First, optodes generally do not provide absolute fluxes in a straightforward way. They measure concentrations (or proxies) at an interface, and converting 2D concentration fields into fluxes requires strong assumptions about geometry, diffusion, and boundary conditions. In soils, these assumptions are often violated by structural complexity and dynamic water distribution. A related limitation is that optodes provide a 2D plane through a 3D system. This is still a major gain over point sensing, but it is not the full spatial truth: processes can be driven by connectivity and gradients extending out of the imaged plane. Furthermore, the presence of an optode foil changes the physical boundary conditions at the interface by so-called "wall effects", creating a diffusion barrier and potentially altering local transport and reaction patterns (Glud et al., 1999). As a result, optodes are best at identifying *where* distinct regimes exist and *how* they evolve, but they must be used cautiously when the goal is to quantify absolute exchange rates or to reconstruct 3D processes.

At the same time, imaging every soil sample in a large treatment experiment is not always necessary or practical. The strength of optodes lies in resolving spatial heterogeneity and revealing mechanisms, whereas many experiments are primarily designed to compare treatment effects across large numbers of samples. Optode imaging produces large datasets by default, and the practical bottleneck quickly shifts from measurement to data handling, particularly in long-term or high-replication studies (Kalinichev et al., 2026). Automated pipelines and machine learning can help with data processing, but they do not remove the need for careful validation: without strong quality control, automated approaches can simply amplify optical artefacts or calibration drift (Zieger and Koren, 2023).

Several soil-specific challenges are also easy to overlook, especially when just starting to integrate optodes into soil experiments. The most fundamental is contact between the optode film and the soil. In dry or structurally unstable soils, air gaps can form. When contact is lost, the sensor starts reporting the changes of the trapped air layer and not the soil itself. This is far less problematic in sediments and waterlogged soils, which helps explain why the transition struggles from aquatic systems, for which optodes were developed, to terrestrial systems. Low moisture content also affects the sensors themselves: many optode chemistries require a hydrated microenvironment, and response times can become slow when the sensing layer dehydrates.

Beyond the soil/sensor interface, optodes are vulnerable to optical artefacts and low-signal scenarios. Dark, organic-rich soils can absorb excitation/emission light and show autofluorescence; illumination gradients, camera drift, material degradation, and photobleaching can generate apparent "chemical patterns" that are purely optical. Therefore, validation, referencing, post-experiment checks, calibration, and (re)calibration should play a crucial role in managing these risks and in separating true soil chemistry from measurement artefacts. A practical overview of the most common technical limitations encountered in soil optode imaging and possible mitigation strategies is summarized in Box A.

More generally, proper calibration and a constant awareness of potential artefacts are essential in optode-based imaging. Simple questions often catch the biggest problems early: Is the image saturated? Is the signal-to-noise ratio still acceptable? Did the optical setup change over time (illumination geometry, lamp intensity, ambient light leaks, focus, camera settings)? Does the optode still behave as expected in reference conditions? Any of these factors can create strong artefacts and produce fake "chemical information" that has little to do with reality. Of course, careful calibration and handling are important for all methods, but optode imaging is unusual in how much experimental freedom it offers (something we consider positive) with respect to the used equipment and samples, while giving limited help (built-in quality controls) for inexperienced users. This is where clearer protocols and better standardization can make a real difference, and why recent work has started to push more explicitly toward calibration- (Rasmussen et al., 2026) and resolution- (Zieger et al., 2022) aware best practices.

In summary, optodes are a powerful hammer in soil science, but only for certain tough nails. They shine when the question is about where and when microenvironments form, and when we want to study mechanistic interactions at a small scale. They provide data in time and space, which is rare. At the same time, they are less suited when the primary goal is absolute flux quantification or high-throughput screening of many treatments. Used thoughtfully and combined with complementary methods, as discussed in Sections 4.4 – 4.5, optodes can be more than a visualization tool: they can become a central component of mechanistic soil biogeochemistry. The next step is to translate these strengths into workflows that work beyond controlled lab setups.

6. Prospects: from lab to in-situ monitoring to modeling

If Section 5 was about choosing the right nails for the optode hammer, this section is about building the workshop: what needs to happen so optodes can move from controlled lab demonstrations to routine, *in-situ* soil monitoring and, ultimately, to mechanistic models and decision support.

Despite the clear scientific value of field studies on plant-soil interactions and soil biogeochemistry, published work that *directly* deploys planar optodes in the field remains extremely limited (Bilyera et al., 2022; Siegwart et al., 2026). The main reason is not a lack of interesting questions, but practical barriers: gaining optical access to the soil profile, installing equipment designed for laboratories, and keeping it stable under real-world weather, variable moisture, changing temperatures, and in the presence of fauna.

Box A
Technical limitations and mitigation strategies for planar optodes in soils

Technical limitation	What to do
Wall effect/boundary disturbance: foil changes the transport of analytes; diffusion biases	**Validate** with orthogonal probes (microsensors) at selected points; interpret gradients near the foil cautiously.
Optical heterogeneity and soil color: absorption, autofluorescence, uneven illumination	**Dual-dye referencing**, dark frames, shielding from stray light; optional optical insulation/scattering layer when compatible.
Moisture dependence (pH, CO_2, NH_3): slow/invalid response in dry or patchy hydration	Ensure **hydration/contact**, monitor moisture state, and treat very dry-soil data as qualitative unless validated
Volatile analytes (NH_3, CO_2) and leakages in **open systems**: losses, solubility, "stickiness"	Use **micro-enclosures**/controlled headspace, close proximity placement, and defined time-window interpretation
Field constraints: drift, changing light/temperature, long deployments	Controlled imaging (dark chamber), reference patches, and **periodic (re)calibration**

In aquatic and marine sediments, specialized *in-situ* equipment for chemical imaging has been used for decades (Glud et al., 2001). For soils, comparable capabilities have only started to emerge recently. A key step forward is the development of standalone, field-deployable imaging systems such as MARTINIS (Multi Analyte Real-Time IN-situ Imaging System) (Rasmussen et al., 2025); see Fig. 1 for a conceptual drawing. These systems make it realistic to monitor soil chemistry over long periods, capturing conditions that are hard (or impossible) to replicate in the lab: diurnal temperature cycles, wetting/drying sequences, freezing/thawing dynamics, and seasonal transitions that often dominate soil biogeochemical function (Wagner-Riddle et al., 2017; Harris et al., 2021). In other words, field-deployable imaging does not just "repeat lab experiments outdoors"; it opens a different class of questions, for example, about timing or recovery of microenvironments.

Going into the field also creates a new set of challenges that can influence the next generation of experiments. A single installation rarely represents a whole landscape: land topography and local hydrology can lead to very different O_2 and moisture regimes over short distances (Elberling et al., 2023). One obvious answer is sensor networks, multiple imaging units that capture heterogeneity and provide replication, but this only becomes feasible if systems remain affordable and easy to maintain. Here, the recent push toward low-cost hardware is encouraging: systems like MARTINIS are reported to be in the range of ~500 – 600 € per unit, which makes replication and network-based designs realistic for many groups (Rasmussen et al., 2025). Still, long-term field deployment quickly turns into an operations problem: power supply, data storage, sensor drift, and maintenance schedules can become as important as the sensor chemistry itself.

Internet-of-Things (IoT) approaches can reduce manual workload by enabling remote monitoring, automated data transfer, cloud-based processing, and early detection of drift or failures, especially when multiple units run in parallel (Capella et al., 2020; Hurst et al., 2026). In parallel, further innovation in multiparameter sensing is likely to increase the scientific value of each deployment. Recent developments, such as grid optodes (Kalinichev et al., 2025) (discussed in Section 4.1) point towards multiparameter imaging becoming more conventional, allowing several parameters to be measured together within the same field workflow.

One of the long-term payoffs of this transition is better models and better decisions. Field-ready optode datasets can provide mechanistic constraints on how microscale spatiotemporal processes scale up to ecosystem behavior, and thereby strengthen process-based modeling frameworks (Groffman et al., 2009; Butterbach-Bahl et al., 2013; Wang et al., 2021). The most powerful designs will likely combine multiparameter optode imaging with measurements of greenhouse gas emissions and nutrient losses, directly connecting "what happens in the soil" to "what leaves the soil." If done well, this can support agricultural management strategies that maintain yield while reducing N losses and greenhouse gas emissions. This is what can move optodes from a mechanistic research tool toward a contributor to decision support.

In short, the future of planar optodes in soils will be shaped by a co-evolution of three things: (I) field deployable imaging systems, (II) more robust and multiparameter sensing approaches, and (III) data workflows that make long-term deployment and model integration practical. Turning these developments into routine tools for soil science will require coordinated methodological progress; key priorities are summarized in Box B.

7. Conclusion

Optodes are powerful and intriguing tools in soil science, and it is evident that we have only begun to explore their full potential. Future developments are likely to expand their impact even further. Improved integration with complementary techniques, the development of new optodes targeting additional analytes, and advances in multianalyte imaging represent particularly promising directions. Another exciting frontier lies in moving optode applications beyond controlled laboratory environments and into field settings, where they can capture soil processes under more realistic conditions.

The aim of this perspective was to provide a clear and honest overview of what optodes can – and cannot – currently achieve. While optodes cannot, in isolation, answer all the complex questions we face in soil science, they can be remarkably powerful when applied thoughtfully and in combination with other approaches. Used wisely, optodes have the potential to become invaluable tools for advancing our understanding of soil processes.

Box B
Wish-list for soil optode imaging routine

Tier 1 | NOW | Reproducibility

- **Open protocols:** soil-specific workflows for contact checks, hydration, calibration, drift control, reporting.
- **Shared calibration datasets:** raw images, metadata, scripts.

Tier 2 | NEXT | Comparability

- **Benchmark soils:** agreed test soils that stress the method (dark organic soils, low moisture, variable ionic strength, strong heterogeneity) with reference measurements
- **Cross-lab intercomparisons:** identical foils and benchmark soils to quantify between-lab variability and identify its sources (optics, calibration, processing, soil handling)

Tier 3 | THEN | Adoption

- **Practical SOPs:** robust, low-friction routines that non-specialists can run without "expert tuning"
- **Standards and uptake:** guidelines aligned with monitoring needs, longer-term standardization frameworks
- **Impact:** integration into management and decision-support workflows

CRediT authorship contribution statement

Pauline Sophie Rummel: Conceptualization, Writing – original draft, Writing – review & editing. **Ya Jie Knöbl:** Conceptualization, Writing – original draft, Writing – review & editing. **Martin Reinhard Rasmussen:** Conceptualization, Writing – original draft, Writing – review & editing. **Klaus Koren:** Conceptualization, Writing – original draft, Writing – review & editing. **Andrey V. Kalinichev:** Conceptualization, Writing – original draft, Writing – review & editing.

Declaration of competing interest

The authors declare the following financial interests/personal relationships which may be considered as potential competing interests: Klaus Koren reports financial support was provided by Villum Foundation. Klaus Koren reports financial support was provided by Poul Due Jensen Foundation. Klaus Koren reports financial support was provided by Danish National Research Foundation. Andrey V. Kalinichev reports financial support was provided by Aarhus University Aarhus Institute of Advanced Studies. Andrey V. Kalinichev reports financial support was provided by Aarhus Universitets Forskningsfond. Pauline Sophie Rummel reports financial support was provided by Novo Nordisk Foundation. If there are other authors, they declare that they have no known competing financial interests or personal relationships that could have appeared to influence the work reported in this paper.

Acknowledgement

The authors would like to thank the following funding sources for supporting our work: Villum Fonden (VIL50075) (KK), Grundfos foundation (KK), Independent Reseach Fund Denmark (DFF-5244-00102B), AIAS-AUFF Fellowship from the Aarhus Institute of Advanced Studies (AIAS), Aarhus Universitets Forskningsfond (AUFF) (AVK), the Pioneer Center for Research in Sustainable Agricultural Futures (Land-CRAFT, DNRF grant number P2) (KK), and Novo Nordisk Fonden (NNF) Postdoctoral Fellowship (grant number NNF22OC0079335) (PSR).

A special thanks to Lise Ryø Hedegaard for drawing the conceptual figures.

References

Abel, T., Ungerböck, B., Klimant, I., Mayr, T., 2012. Fast responsive, optical trace level ammonia sensor for environmental monitoring. Chemistry Central Journal 6, 124. https://doi.org/10.1186/1752-153X-6-124.

Ameer, S., Ibrahim, H., Kulsoom, F.N.U., Ameer, G., Sher, M., 2024. Real-time detection and measurements of nitrogen, phosphorous & potassium from soil samples: a comprehensive review. Journal of Soils and Sediments 24, 2565–2583. https://doi.org/10.1007/s11368-024-03827-5.

Angst, G., Mueller, K.E., Nierop, K.G.J., Simpson, M.J., 2021. Plant- or microbial-derived? A review on the molecular composition of stabilized soil organic matter. Soil Biology and Biochemistry 156, 108189. https://doi.org/10.1016/j.soilbio.2021.108189.

Askaer, L., Elberling, B., Glud, R.N., Kühl, M., Lauritsen, F.R., Joensen, H.P., 2010. Soil heterogeneity effects on O2 distribution and CH4 emissions from wetlands: *in Situ* and mesocosm studies with planar O2 optodes and membrane inlet mass spectrometry. Soil Biology and Biochemistry 42, 2254–2265. https://doi.org/10.1016/j.soilbio.2010.08.026.

Bartram, A.K., Jiang, X., Lynch, M.D.J., Masella, A.P., Nicol, G.W., Dushoff, J., Neufeld, J.D., 2014. Exploring links between pH and bacterial community composition in soils from the Craibstone Experimental Farm. FEMS Microbiology Ecology 87, 403–415. https://doi.org/10.1111/1574-6941.12231.

Bateman, E.J., Baggs, E.M., 2005. Contributions of nitrification and denitrification to N2O emissions from soils at different water-filled pore space. Biology and Fertility of Soils 41, 379–388. https://doi.org/10.1007/s00374-005-0858-3.

Behera, S.N., Sharma, M., Aneja, V.P., Balasubramanian, R., 2013. Ammonia in the atmosphere: a review on emission sources, atmospheric chemistry and deposition on terrestrial bodies. Environmental Science and Pollution Research 20, 8092–8131. https://doi.org/10.1007/s11356-013-2051-9.

Bereswill, S., Rudolph-Mohr, N., Oswald, S.E., 2024. Spatio-temporal patterns of rhizosphere CO2 concentration are linked to root type and soil moisture dynamics in white lupine. Rhizosphere 29, 100857. https://doi.org/10.1016/j.rhisph.2024.100857.

Bilyera, N., Hummel, C., Daudin, G., Santangeli, M., Zhang, X., Santner, J., Lippold, E., Schlüter, S., Bertrand, I., Wenzel, W., Spielvogel, S., Vetterlein, D., Razavi, B.S., Oburger, E., 2022. Co-localised phosphorus mobilization processes in the rhizosphere of field-grown maize jointly contribute to plant nutrition. Soil Biology and Biochemistry 165, 108497. https://doi.org/10.1016/j.soilbio.2021.108497.

Bilyera, N., Kuzyakov, Y., 2024. Soil zymography: a decade of rapid development in microbial hotspot imaging. Soil Biology and Biochemistry 189, 109264. https://doi.org/10.1016/j.soilbio.2023.109264.

Blossfeld, S., Gansert, D., Thiele, B., Kuhn, A.J., Lösch, R., 2011. The dynamics of oxygen concentration, pH value, and organic acids in the rhizosphere of Juncus spp. Soil Biology and Biochemistry 43, 1186–1197. https://doi.org/10.1016/j.soilbio.2011.02.007.

Blossfeld, S., Schreiber, C.M., Liebsch, G., Kuhn, A.J., Hinsinger, P., 2013. Quantitative imaging of rhizosphere pH and CO2 dynamics with planar optodes. Annals of Botany 112, 267–276. https://doi.org/10.1093/aob/mct047.

Blossfeld, S., Gansert, D., 2007. A novel non-invasive optical method for quantitative visualization of pH dynamics in the rhizosphere of plants. Plant, Cell and Environment 30, 176–186. https://doi.org/10.1111/j.1365-3040.2006.01616.x.

Blossfeld, S., Gansert, D., 2012. The use of planar optodes in root studies for quantitative imaging. In: Mancuso, S. (Ed.), Measuring Roots: an Updated Approach. Springer, Berlin, Heidelberg, pp. 83–92. https://doi.org/10.1007/978-3-642-22067-8_5.

Bognár, Z., Mosshammer, M., Brodersen, K.E., Bollati, E., Gyurcsányi, R.E., Kühl, M., 2024. Multiparameter sensing of oxygen and pH at biological interfaces via hyperspectral imaging of luminescent sensor nanoparticles. ACS Sensors 9, 1763–1774. https://doi.org/10.1021/acssensors.3c01941.

Borisov, S.M., Neurauter, G., Schroeder, C., Klimant, I., Wolfbeis, O.S., 2006. Modified dual lifetime referencing method for simultaneous optical determination and sensing of two analytes. Applied Spectroscopy 60, 1167–1173. https://doi.org/10.1366/000370206778664590.

Bornø, M.L., Zervas, A., Bak, F., Merl, T., Koren, K., Nicolaisen, M.H., Jensen, L.S., Müller-Stöver, D.S., 2023. Differential impacts of sewage sludge and biochar on phosphorus-related processes: an imaging study of the rhizosphere. The Science of the Total Environment 905, 166888. https://doi.org/10.1016/j.scitotenv.2023.166888.

Bååth, E., 1996. Adaptation of soil bacterial communities to prevailing pH in different soils. FEMS Microbiology Ecology 19, 227–237. https://doi.org/10.1111/j.1574-6941.1996.tb00215.x.

Buss, W., Shepherd, J.G., Heal, K.V., Mašek, O., 2018. Spatial and temporal microscale pH change at the soil-biochar interface. Geoderma 331, 50–52. https://doi.org/10.1016/j.geoderma.2018.06.016.

Butterbach-Bahl, K., Baggs, E.M., Dannenmann, M., Kiese, R., Zechmeister-Boltenstern, S., 2013. Nitrous oxide emissions from soils: how well do we understand the processes and their controls. Philosophical Transactions of the Royal Society B 368, 1–13. https://doi.org/10.1098/rstb.2013.0122.

Capella, J.V., Bonastre, A., Campelo, J.C., Ors, R., Peris, M., 2020. IoT & environmental analytical chemistry: towards a profitable symbiosis. Trends in Environmental Analytical Chemistry 27, e00095. https://doi.org/10.1016/j.teac.2020.e00095.

Chen, X., Gu, F., Zhang, D., Lin, W., Tang, J., Zhang, B., Yu, X., 2024. Investigating the two-dimensional distribution of soil pH and phosphorus in the charosphere: a short-term incubation experiment. Agronomy 14. https://doi.org/10.3390/agronomy14122907.

Damala, P., Zdrachek, E., Bakker, E., 2023. Commercially available nitrate ionophores in potentiometric sensors are not superior to common ion-exchangers. Electroanalysis 35, e202200247. https://doi.org/10.1002/elan.202200247.

Davison, W. (Ed.), 2016. Diffusive Gradients in Thin-Films for Environmental Measurements, Cambridge Environmental Chemistry Series. Cambridge University Press, Cambridge. https://doi.org/10.1017/CBO9781316442654.

Davison, William, Zhang, Hao, Warnken, Kent W., 2007. Chapter 16 theory and applications of DGT measurements in soils and sediments. In: Comprehensive Analytical Chemistry. Elsevier, pp. 353–378. https://doi.org/10.1016/S0166-526X(06)48016-8.

Dawson, J.J.C., Billett, M.F., Hope, D., 2001. Diurnal variations in the carbon chemistry of two acidic peatland streams in north-east Scotland. Freshwater Biology 46, 1309–1322. https://doi.org/10.1046/j.1365-2427.2001.00751.x.

Delin, S., Strömberg, N., 2011. Imaging-optode measurements of ammonium distribution in soil after different manure amendments. European Journal of Soil Science 62, 295–304. https://doi.org/10.1111/j.1365-2389.2010.01326.x.

Dotaniya, M.L., Meena, V.D., 2015. Rhizosphere effect on nutrient availability in soil and its uptake by plants: a review. Proceedings of the National Academy of Sciences, India - Section B: Biological Sciences 85, 1–12. https://doi.org/10.1007/s40011-013-0297-0.

El-Shatnawi, M.K.J., Makhadmeh, I.M., 2001. Ecophysiology of the plant–rhizosphere System. Journal of Agronomy and Crop Science 187, 1–9. https://doi.org/10.1046/j.1439-037X.2001.00498.x.

Elberling, B.B., Kovács, G.M., Hansen, H.F.E., Fensholt, R., Ambus, P., Tong, X., Gominski, D., Mueller, C.W., Poultney, D.M.N., Oehmcke, S., 2023. High nitrous oxide emissions from temporary flooded depressions within croplands. Communications Earth & Environment 4, 463. https://doi.org/10.1038/s43247-023-01095-8.

Fan, Y., Zhu, Q., Aller, R.C., Rhoads, D.C., 2011. An in situ multispectral Imaging System for planar optodes in sediments: examples of high-resolution seasonal patterns of pH. Aquatic Geochemistry 17, 457–471. https://doi.org/10.1007/s10498-011-9124-5.

Fernández-García, V., Miesel, J., Baeza, M.J., Marcos, E., Calvo, L., 2019. Wildfire effects on soil properties in fire-prone pine ecosystems: indicators of burn severity legacy over the medium term after fire. Applied Soil Ecology 135, 147–156. https://doi.org/10.1016/j.apsoil.2018.12.002.

Fierer, N., Jackson, R.B., 2006. The diversity and biogeography of soil bacterial communities. Proceedings of the National Academy of Sciences 103, 626–631. https://doi.org/10.1073/pnas.0507535103.

Findlay, Stuart E.G., Hamilton, Stephen K., Strayer, David L., Weathers, Kathleen C., 2021. Microbially mediated redox reactions. In: Fundamentals of Ecosystem Science. Academic Press, pp. 103–111. https://doi.org/10.1016/B978-0-12-812762-9.00005-8.

Franklin, R.B., Mills, A.L., 2009. Importance of spatially structured environmental heterogeneity in controlling microbial community composition at small spatial scales in an agricultural field. Soil Biology and Biochemistry 41, 1833–1840. https://doi.org/10.1016/j.soilbio.2009.06.003.

Ge, Y., Ying, K., Zhang, S., Wang, S., Fang, Y., Huang, J., Lin, H., Xu, T., Yu, G., 2025. Planar optode imaging reveals spatio-temporal heterogeneity of rhizosphere microecology in Celosia argentea under cadmium stress. Toxics 14. https://doi.org/10.3390/toxics14010034.

Glud, R.N., Kühl, M., Kohls, O., Ramsing, N.B., 1999. Heterogeneity of oxygen production and consumption in a photosynthetic microbial mat as studied by planar optodes. Journal of Phycology 35, 270–279. https://doi.org/10.1046/j.1529-8817.1999.3520270.x.

Glud, R.N., Ramsing, N.B., Gundersen, J.K., Klimant, I., 1996. Planar optrodes: a new tool for fine scale measurements of two-dimensional O2 distribution in benthic communities. Marine Ecology Progress Series 140, 217–226. https://doi.org/10.3354/meps140217.

Glud, R.N., Tengberg, A., Kühl, M., Hall, P.O.J., Klimant, I., 2001. An in situ instrument for planar O2 optode measurements at benthic interfaces. Limnology and Oceanography 46, 2073–2080. https://doi.org/10.4319/lo.2001.46.8.2073.

Gómez-Rey, M.X., Couto-Vázquez, A., García-Marco, S., González-Prieto, S.J., 2013. Impact of fire and post-fire management techniques on soil chemical properties. Geoderma 195–196, 155–164. https://doi.org/10.1016/j.geoderma.2012.12.005.

Goulding, K.W.T., 2016. Soil acidification and the importance of liming agricultural soils with particular reference to the United Kingdom. Soil Use and Management 32, 390–399. https://doi.org/10.1111/sum.12270.

Groffman, P.M., Butterbach-Bahl, K., Fulweiler, R.W., Gold, A.J., Morse, J.L., Stander, E. K., Tague, C., Tonitto, C., Vidon, P., 2009. Challenges to incorporating spatially and temporally explicit phenomena (hotspots and hot moments) in denitrification models. Biogeochemistry 93, 49–77. https://doi.org/10.1007/s10533-008-9277-5.

Han, C., Yao, L., Xu, D., Xie, X., Zhang, C., 2016. High-resolution imaging of pH in alkaline sediments and water based on a new rapid response Fluorescent Planar optode. Scientific Reports 6, 26417. https://doi.org/10.1038/srep26417.

Harper, L.A., Catchpoole, V.R., Davis, R., Weir, K.L., 1983. Ammonia volatilization: soil, plant, and microclimate effects on diurnal and seasonal fluctuations. Agronomy Journal 75, 212–218. https://doi.org/10.2134/agronj1983.00021962007500020014x.

Harris, E., Diaz-Pines, E., Stoll, E., Schloter, M., Schulz, S., Duffner, C., Li, K., Moore, K.L., Ingrisch, J., Reinthaler, D., Zechmeister-Boltenstern, S., Glatzel, S., Brüggemann, N., Bahn, M., 2021. Denitrifying pathways dominate nitrous oxide emissions from managed grassland during drought and rewetting. Science Advances 7. https://doi.org/10.1126/sciadv.abb7118.

Heitkötter, J., Marschner, B., 2018. Soil zymography as a powerful tool for exploring hotspots and substrate limitation in undisturbed subsoil. Soil Biology and Biochemistry 124, 210–217. https://doi.org/10.1016/j.soilbio.2018.06.021.

Helliwell, J.R., Sturrock, C.J., Grayling, K.M., Tracy, S.R., Flavel, R.J., Young, I.M., Whalley, W.R., Mooney, S.J., 2013. Applications of X-ray computed tomography for examining biophysical interactions and structural development in soil systems: a review. European Journal of Soil Science 64, 279–297. https://doi.org/10.1111/ejss.12028.

Hoefer, C., Santner, J., Borisov, S.M., Wenzel, W.W., Puschenreiter, M., 2017. Integrating chemical imaging of cationic trace metal solutes and pH into a single hydrogel layer. Analytica Chimica Acta 950, 88–97. https://doi.org/10.1016/j.aca.2016.11.004.

Holz, M., Becker, J.N., Daudin, G., Oburger, E., 2020. Application of planar optodes to measure CO2 gradients in the rhizosphere of unsaturated soils. Rhizosphere 16, 100266. https://doi.org/10.1016/j.rhisph.2020.100266.

Honeyman, A.S., Merl, T., Spear, J.R., Koren, K., 2023. Optode-based chemical imaging of laboratory burned soil reveals millimeter-scale heterogeneous biogeochemical responses. Environmental Research 224, 115469. https://doi.org/10.1016/j.envres.2023.115469.

Hu, Y., Merl, T., Pedersen, J., Bornø, M.L., Tariq, A., Koren, K., Sommer, S.G., 2024. Tracing N2O from dairy processing sludge amended soil with visualizing microscale heterogeneity of NH3 and pH (Short Communication). Atmospheric Environment X 23, 100283. https://doi.org/10.1016/j.aeaoa.2024.100283.

Hurst, A., Kalinichev, A.V., Koren, K., Lucani, D.E., 2026. Not all those who drift are lost: drift correction and calibration scheduling for the IoT. IEEE Internet of Things Journal 13, 2144–2154. https://doi.org/10.1109/JIOT.2025.3628204.

Kalinichev, A.V., Lucani, D.E., Koren, K., 2026. From the ground to the data cloud: what limits chemical sensor networks from reaching their full potential and what can be done to overcome those chal-lenges. TrAC, Trends in Analytical Chemistry, 118969. https://doi.org/10.1016/j.trac.2026.118969.

Kalinichev, A.V., Rasmussen, M.R., Hoch, F.L., Parnicka, Z., Fiutowski, J., Koren, K., Kunstmann-Olsen, C., 2025. Spatially patterned grid optodes for simultaneous multiparameter chemical imaging. ACS Sensors 10, 8498–8508. https://doi.org/10.1021/acssensors.5c02007.

Kalinichev, A.V., Zieger, S.E., Koren, K., 2023. Optical sensors (optodes) for multiparameter chemical imaging: classification, challenges, and prospects. The Analyst 149, 29–45. https://doi.org/10.1039/D3AN01661G.

Kassal, P., Sigurnjak, M., Steinberg, I.M., 2019. Paper-based ion-selective optodes for continuous sensing: reversible potassium ion monitoring. Talanta 193, 51–55. https://doi.org/10.1016/j.talanta.2018.09.031.

Keiluweit, M., Gee, K., Denney, A., Fendorf, S., 2018. Anoxic microsites in upland soils dominantly controlled by clay content. Soil Biology and Biochemistry 118, 42–50. https://doi.org/10.1016/j.soilbio.2017.12.002.

Keiluweit, M., Nico, P.S., Kleber, M., Fendorf, S., 2016. Are oxygen limitations under recognized regulators of organic carbon turnover in upland soils? Biogeochemistry 127, 157–171. https://doi.org/10.1007/s10533-015-0180-6.

Keiluweit, M., Wanzek, T., Kleber, M., Nico, P., Fendorf, S., 2017. Anaerobic microsites have an unaccounted role in soil carbon stabilization. Nature Communications 8, 1771. https://doi.org/10.1038/s41467-017-01406-6.

Kim, M., Or, D., 2019. Microscale pH variations during drying of soils and desert biocrusts affect HONO and NH3 emissions. Nature Communications 10, 3944. https://doi.org/10.1038/s41467-019-11956-6.

Kissel, D.E., Cabrera, M.L., Paramasivam, S., 2008. Ammonium, Ammonia, and urea reactions in Soils. In: Nitrogen in Agricultural Systems. John Wiley & Sons, Ltd, pp. 101–155. https://doi.org/10.2134/agronmonogr49.c4.

Klimant, I., Meyer, V., Kühl, M., 1995. Fiber-optic oxygen microsensors, a new tool in aquatic biology. Limnology and Oceanography 40, 1159–1165. https://doi.org/10.4319/lo.1995.40.6.1159.

Koop-Jakobsen, K., Meier, R.J., Mueller, P., 2021. Plant-Mediated rhizosphere oxygenation in the native invasive Salt Marsh Grass Elymus athericus. Frontiers in Plant Science 12. https://doi.org/10.3389/fpls.2021.669751.

Koop-Jakobsen, K., Mueller, P., Meier, R.J., Liebsch, G., Jensen, K., 2018. Plant-sediment interactions in salt marshes – an optode imaging study of O2, pH, and CO2 gradients in the rhizosphere. Frontiers in Plant Science 9, 1–11. https://doi.org/10.3389/fpls.2018.00541.

Koop-Jakobsen, K., Wenzhöfer, F., 2015. The dynamics of plant-mediated sediment oxygenation in Spartina anglica Rhizospheres—A planar optode Study. Estuaries and Coasts 38, 951–963. https://doi.org/10.1007/s12237-014-9861-y.

Koren, K., Kühl, M., 2015. A simple laminated paper-based sensor for temperature sensing and imaging. Sensors and Actuators B: Chemical 210, 124–128. https://doi.org/10.1016/j.snb.2014.12.102.

Koren, K., Zieger, S.E., 2021. Optode based chemical imaging—Possibilities, challenges, and new avenues in multidimensional optical sensing. ACS Sensors 6, 1671–1680. https://doi.org/10.1021/acssensors.1c00480.

Kuzyakov, Y., Blagodatskaya, E.V., 2015. Microbial hotspots and hot moments in soil: concept & review. Soil Biology and Biochemistry 83, 184–199. https://doi.org/10.1016/j.soilbio.2015.01.025.

Lacroix, E.M., Aeppli, M., Boye, K., Brodie, E., Fendorf, S., Keiluweit, M., Naughton, H.R., Noël, V., Sihi, D., 2023. Consider the anoxic microsite: acknowledging and appreciating spatiotemporal redox heterogeneity in soils and sediments. ACS Earth and Space Chemistry 7, 1592–1609. https://doi.org/10.1021/acsearthspacechem.3c00032.

Larsen, M., Santner, J., Oburger, E., Wenzel, W.W., Glud, R.N., 2015. O2 dynamics in the rhizosphere of young rice plants (Oryza sativa L.) as studied by planar optodes. Plant and Soil 390, 279–292. https://doi.org/10.1007/s11104-015-2382-z.

Lehto, N.J., Larsen, M., Zhang, H., Glud, R.N., Davison, W., 2017. A mesocosm study of oxygen and trace metal dynamics in sediment microniches of reactive organic material. Scientific Reports 7, 11369. https://doi.org/10.1038/s41598-017-10179-3.

Lenzewski, N., Mueller, P., Meier, R.J., Liebsch, G., Jensen, K., Koop-Jakobsen, K., 2018. Dynamics of oxygen and carbon dioxide in rhizospheres of Lobelia dortmanna – a planar optode study of belowground gas exchange between plants and sediment. New Phytologist 218, 131–141. https://doi.org/10.1111/nph.14973.

Li, C., Ding, S., Yang, L., Zhu, Q., Chen, M., Tsang, D.C.W., Cai, G., Feng, C., Wang, Y., Zhang, C., 2019. Planar optode: a two-dimensional imaging technique for studying spatial-temporal dynamics of solutes in sediment and soil. Earth-Science Reviews 197, 102916. https://doi.org/10.1016/j.earscirev.2019.102916.

Liu, H., Chi, L., Shen, J., Arandiyan, H., Wang, Y., Wang, X., 2024. Principles, applications, and limitations of diffusive gradients in thin films induced fluxed in soils and sediments. Chemosphere 350, 141061. https://doi.org/10.1016/j.chemosphere.2023.141061.

Lombi, E., Doolette, C.L., da Silva, R.C., McKenna, B.A., Kopittke, P.M., 2025. Unveiling chemical gradients in the fertosphere: a paradigm shift to enhance fertilizer efficiency and decrease the environmental impact of overfertilisation. Environmental Science & Technology 59, 14853–14861. https://doi.org/10.1021/acs.est.5c04757.

Lussich, F., Dhaliwal, J.K., Faiia, A.M., Jagadamma, S., Schaeffer, S.M., Saha, D., 2024. Cover crop residue decomposition triggered soil oxygen depletion and promoted nitrous oxide emissions. Scientific Reports 14, 8437. https://doi.org/10.1038/s41598-024-58942-7.

Ma, X., Liu, Y., Shen, W., Kuzyakov, Y., 2021. Phosphatase activity and acidification in lupine and maize rhizosphere depend on phosphorus availability and root properties: coupling zymography with planar optodes. Applied Soil Ecology 167, 104029. https://doi.org/10.1016/j.apsoil.2021.104029.

Maslow, A., 1966. The Psychology of Science: a Reconnaissance. New York.

Merl, T., Hu, Y., Pedersen, J., Zieger, S.E., Bornø, M.L., Tariq, A., Sommer, S.G., Koren, K., 2023. Optical Chemical Sensors for Soil Analysis: possibilities and Challenges of Visualizing NH3 concentrations as well as pH and O2 Microscale Heterogeneity. Environmental Sciences: Advances 00 1–10. https://doi.org/10.1039/D3VA00127J.

Merl, T., Rasmussen, M.R., Koch, L.R., Søndergaard, J.V., Bust, F.F., Koren, K., 2022. Measuring soil pH at in situ like conditions using optical pH sensors (pH-optodes).

Soil Biology and Biochemistry 175, 4–6. https://doi.org/10.1016/j.soilbio.2022.108862.
Merl, T., Sedlacek, C.J., Pjevac, P., Fuchslueger, L., Sandén, T., Spiegel, H., Koren, K., Giguere, A.T., 2024. Visualizing small-scale subsurface NH3 and pH dynamics surrounding nitrogen fertilizer granules and impacts on nitrification activity. Soil Biology and Biochemistry 189. https://doi.org/10.1016/j.soilbio.2023.109273.
Merl, T., Koren, K., 2020. Visualizing NH3 emission and the local O2 and pH microenvironment of soil upon manure application using optical sensors. Environment International 144, 106080. https://doi.org/10.1016/j.envint.2020.106080.
Mills, A., Chang, Q., 1993. Fluorescence plastic thin-film sensor for carbon dioxide. The Analyst 118, 839–843. https://doi.org/10.1039/AN9931800839.
Moßhammer, M., Scholz, V.V., Holst, G., Kühl, M., Koren, K., 2019. Luminescence lifetime imaging of O2 with a frequency-domain-based camera System. Journal of Visualized Experiments, e60191. https://doi.org/10.3791/60191.
Moßhammer, M., Strobl, M., Kühl, M., Klimant, I., Borisov, S.M., Koren, K., 2016. Design and application of an optical sensor for simultaneous imaging of pH and dissolved O2 with low cross-talk. ACS Sensors 1, 681–687. https://doi.org/10.1021/acssensors.6b00071.
Muñoz-Rojas, M., Erickson, T.E., Martini, D., Dixon, K.W., Merritt, D.J., 2016. Soil physicochemical and microbiological indicators of short, medium and long term post-fire recovery in semi-arid ecosystems. Ecological Indicators 63, 14–22. https://doi.org/10.1016/j.ecolind.2015.11.038.
Natta, G., Merl, T., Laini, A., Roggero, A., Rolando, A., Palestrini, C., Koren, K., Marzocchi, U., 2025. Planar optodes reveal spatiotemporal heterogeneity of oxic and pH microenvironments driven by dung beetle activity in soil. Soil Biology and Biochemistry 211, 109965. https://doi.org/10.1016/j.soilbio.2025.109965.
Neumann, G., Römheld, V., 2012. Chapter 14 - rhizosphere chemistry in relation to plant nutrition. In: Marschner, P. (Ed.), Marschner's Mineral Nutrition of Higher Plants, third ed. Academic Press, San Diego, pp. 347–368. https://doi.org/10.1016/B978-0-12-384905-2.00014-5.
Nguyen, Q.V., Wu, D., Kong, X., Bol, R., Petersen, S.O., Jensen, L.S., Liu, S., Brüggemann, N., Glud, R.N., Larsen, M., Bruun, S., 2017. Effects of cattle slurry and nitrification inhibitor application on spatial soil O2 dynamics and N2O production pathways. Soil Biology and Biochemistry 114, 200–209. https://doi.org/10.1016/j.soilbio.2017.07.012.
Nishimura, S., Yonemura, S., Minamikawa, K., Yagi, K., 2015. Seasonal and diurnal variations in net carbon dioxide flux throughout the year from soil in paddy field. Journal of Geophysical Research, Biogeosciences 120, 63–76. https://doi.org/10.1002/2014JG002746.
Pedersen, L.L., Dechesne, A., Smets, B.F., 2015. A nitrate sensitive planar optode; performance and interferences. Talanta 144, 933–937. https://doi.org/10.1016/j.talanta.2015.07.046.
Polerecky, L., Volkenborn, N., Stief, P., 2006. High temporal resolution oxygen imaging in bioirrigated sediments. Environmental Science & Technology 40, 5763–5769. https://doi.org/10.1021/es060494l.
Potdar, R.P., Shirolkar, M.M., Verma, A.J., More, P.S., Kulkarni, A., 2021. Determination of soil nutrients (NPK) using optical methods: a mini review. Journal of Plant Nutrition 44, 1826–1839. https://doi.org/10.1080/01904167.2021.1884702.
Randall, D.J., Tsui, T.K.N., 2002. Ammonia toxicity in fish. Marine Pollution Bulletin 45, 17–23. https://doi.org/10.1016/S0025-326X(02)00227-8.
Rasmussen, M.R., Koren, K., Kalinichev, A.V., 2026. Revisiting camera-based calibration of oxygen optodes: error sources, empirical alternatives, and practical guidelines for end-users. Sensors and Actuators B: Chemical 448, 139030. https://doi.org/10.1016/j.snb.2025.139030.
Rasmussen, M.R., Merl, T., Zieger, S.E., Thomsen, S., Kiese, R., Butterbach-Bahl, K., Koren, K., 2025. A novel, standalone and low-cost system for in-situ chemical imaging with planar optodes in soils. Sensors and Actuators B: Chemical 424, 136894. https://doi.org/10.1016/j.snb.2024.136894.
Razavi, B.S., Zhang, X., Bilyera, N., Guber, A., Zarebanadkouki, M., 2019. Soil zymography: simple and reliable? Review of current knowledge and optimization of the method. Rhizosphere 11, 100161. https://doi.org/10.1016/j.rhisph.2019.100161.
Recous, S., Machet, J.M., Mary, B., 1992. The partitioning of fertilizer-N between soil and crop: Comparison of ammonium and nitrate applications. Plant and Soil 144, 101–111. https://doi.org/10.1007/BF00018850.
Rickelt, L.F., Askaer, L., Walpersdorf, E., Elberling, B., Glud, R.N., Kühl, M., 2013a. An optode sensor array for long-term in situ oxygen measurements in soil and sediment. Journal of Environmental Quality 42, 1267–1273. https://doi.org/10.2134/jeq2012.0334.
Rickelt, L.F., Askaer, L., Walpersdorf, E., Elberling, B., Glud, R.N., Kühl, M., 2013b. An optode sensor array for long-term in situ oxygen measurements in soil and sediment. Journal of Environmental Quality 42, 1267–1273. https://doi.org/10.2134/jeq2012.0334.
Rochette, P., Angers, D.A., Chantigny, M.H., Gasser, M.-O., MacDonald, J.D., Pelster, D. E., Bertrand, N., 2013. NH3 volatilization, soil concentration and soil pH following subsurface banding of urea at increasing rates. Canadian Journal of Soil Science 93, 261–268. https://doi.org/10.4141/cjss2012-095.
Rohe, L., Apelt, B., Vogel, H.-J., Well, R., Wu, G.-M., Schlüter, S., 2021. Denitrification in soil as a function of oxygen availability at the microscale. Biogeosciences 18, 1185–1201. https://doi.org/10.5194/bg-18-1185-2021.
Rudolph, N., Voss, S., Moradi, A.B., Nagl, S., Oswald, S.E., 2013. Spatio-temporal mapping of local soil pH changes induced by roots of lupin and soft-rush. Plant and Soil 369, 669–680. https://doi.org/10.1007/s11104-013-1775-0.
Rummel, P.S., Rasmussen, M.R., Saghaï, A., Merl, T., Hallin, S., Mueller, C.W., Koren, K., 2026. Maize root growth, oxygen and N availability drive formation of N2O hotspots in soil. Geoderma 467, 117734. https://doi.org/10.1016/j.geoderma.2026.117734.
Russenes, A.L., Korsaeth, A., Bakken, L.R., Dörsch, P., 2016. Spatial variation in soil pH controls off-season N2O emission in an agricultural soil. Soil Biology and Biochemistry 99, 36–46. https://doi.org/10.1016/j.soilbio.2016.04.019.
Santner, J., Larsen, M., Kreuzeder, A., Glud, R.N., 2015. Two decades of chemical imaging of solutes in sediments and soils - a review. Analytica Chimica Acta 878, 9–42. https://doi.org/10.1016/j.aca.2015.02.006.
Schlüter, S., Leuther, F., Albrecht, L., Hoeschen, C., Kilian, R., Surey, R., Mikutta, R., Kaiser, K., Mueller, C.W., Vogel, H.-J., 2022. Microscale carbon distribution around pores and particulate organic matter varies with soil moisture regime. Nature Communications 13, 2098. https://doi.org/10.1038/s41467-022-29605-w.
Schmidt-Böcking, H., Reich, K., Templeton, A., Trageser, W., Vill, V., 2016. S10. In: Schmidt-Böcking, H., Reich, K., Templeton, A., Trageser, W., Vill, V. (Eds.), Otto Sterns Veröffentlichungen – Band 2: Sterns Veröffentlichungen Von 1916 Bis 1926. Springer, Berlin, Heidelberg, pp. 79–85. https://doi.org/10.1007/978-3-662-46962-0_5.
Schutting, S., Klimant, I., de Beer, D., Borisov, S.M., 2014. New highly fluorescent pH indicator for ratiometric RGB imaging of pCO2. Methods and Applications in Fluorescence 2, 024001. https://doi.org/10.1088/2050-6120/2/2/024001.
Schwendt, G., Kalinichev, A.V., Borisov, S.M., Koren, K., 2024. Simultaneous imaging of temperature and oxygen by utilizing thermally activated delayed fluorescence and phosphorescence of a single indicator. ACS Measurement Science Au 4, 568–576. https://doi.org/10.1021/acsmeasuresciau.4c00040.
Scotto di Perta, E., Fiorentino, N., Carozzi, M., Cervelli, E., Pindozzi, S., 2020. A review of chamber and micrometeorological methods to quantify NH3 emissions from fertilisers field application. International Journal of Agronomy 2020, 8909784. https://doi.org/10.1155/2020/8909784.
Seiler, K., Morf, W.E., Rusterholz, B., Simon, W., 1989. Design and characterization of a novel ammonium ion selective optical sensor based on neutral ionophores. Analytical Sciences 5, 557–561. https://doi.org/10.2116/analsci.5.557.
Sexstone, A.J., Revsbech, N.P., Parkin, T.B., Tiedje, J.M., 1985. Direct measurement of oxygen profiles and denitrification rates in soil aggregates. Soil Science Society of America Journal 49, 645–651. https://doi.org/10.2136/sssaj1985.03615995004900030024x.
Siegwart, L., Belard, M., Merl, T., Moens, C., Zhu, C., George, T., Koren, K., Dresbøll, D.B., van der Bom, F., 2026. Intercropping alters rhizosphere chemistry but not early root distribution in a low phosphorus field. Plant and Soil. https://doi.org/10.1007/s11104-026-08677-3.
Sommer, S.G., Génermont, S., Cellier, P., Hutchings, N.J., Olesen, J.E., Morvan, T., 2003. Processes controlling ammonia emission from livestock slurry in the field. European Journal of Agronomy 19, 465–486. https://doi.org/10.1016/S1161-0301(03)00037-6.
Song, X., Ju, X., Topp, C.F.E., Rees, R.M., 2019. Oxygen regulates nitrous oxide production directly in agricultural soils. Environmental Science & Technology 53, 12539–12547. https://doi.org/10.1021/acs.est.9b03089.
Spohn, M., Carminati, A., Kuzyakov, Y., 2013. Soil zymography – a novel *in situ* method for mapping distribution of enzyme activity in soil. Soil Biology and Biochemistry 58, 275–280. https://doi.org/10.1016/j.soilbio.2012.12.004.
Strömberg, N., 2008. Determination of ammonium turnover and flow patterns close to roots using imaging optodes. Environmental Science & Technology 42, 1630–1637. https://doi.org/10.1021/es071400q.
Strömberg, N., Hakonen, A., 2011. Plasmophore sensitized imaging of ammonia release from biological tissues using optodes. Analytica Chimica Acta 704, 139–145. https://doi.org/10.1016/j.aca.2011.08.019.
Strobl, M., Walcher, A., Mayr, T., Klimant, I., Borisov, S.M., 2017. Trace Ammonia sensors based on fluorescent near-infrared-emitting aza-BODIPY dyes. Analytical Chemistry 89, 2859–2865. https://doi.org/10.1021/acs.analchem.6b04045.
Susha Lekshmi, S.U., Singh, D.N., Shojaei Baghini, M., 2014. A critical review of soil moisture measurement. Measurement 54, 92–105. https://doi.org/10.1016/j.measurement.2014.04.007.
Tao, J., Fan, L., Jiang, T., Song, X., Zhao, M., Zhou, J., Kuzyakov, Y., Zamanian, K., 2025. *In situ* visualization of soil profile acidification and processes following nitrogen fertilization and liming. Geoderma 456, 117243. https://doi.org/10.1016/j.geoderma.2025.117243.
Thomson, A.J., Giannopoulos, G., Pretty, J., Baggs, E.M., Richardson, D.J., 2012. Biological sources and sinks of nitrous oxide and strategies to mitigate emissions. Philosophical Transactions of the Royal Society B: Biological Sciences 367, 1157–1168. https://doi.org/10.1098/rstb.2011.0415.
Timmer, B., Olthuis, W., van den Berg, A., 2005. Ammonia sensors and their applications—a review. Sensors and Actuators B: Chemical 107, 666–677. https://doi.org/10.1016/j.snb.2004.11.054.
Wagner-Riddle, C., Congreves, K.A., Abalos, D., Berg, A.A., Brown, S.E., Ambadan, J.T., Gao, X., Tenuta, M., 2017. Globally important nitrous oxide emissions from croplands induced by freeze–thaw cycles. Nature Geoscience 10, 279–283. https://doi.org/10.1038/ngeo2907.
Waich, K., Mayr, T., Klimant, I., 2007. Microsensors for detection of ammonia at ppb-concentration levels. Measurement Science and Technology 18, 3195. https://doi.org/10.1088/0957-0233/18/10/S22.
Wang, C., Amon, B., Schulz, K., Mehdi, B., 2021. Factors that influence nitrous oxide emissions from agricultural soils as well as their representation in simulation models. Revista Agronomica 11. https://doi.org/10.3390/agronomy11040770.
Wang, C., Zhou, X., Guo, D., Zhao, J., Yan, L., Feng, G., Gao, Q., Yu, H., Zhao, L., 2019. Soil pH is the primary factor driving the distribution and function of microorganisms

in farmland soils in northeastern China. Annals of Microbiology 69, 1461–1473. https://doi.org/10.1007/s13213-019-01529-9.

Wang, H., Yan, Z., Ju, X., Song, X., Zhang, J., Li, S., Zhu-Barker, X., 2023. Quantifying nitrous oxide production rates from nitrification and denitrification under various moisture conditions in agricultural soils: laboratory study and literature synthesis. Frontiers in Microbiology 13. https://doi.org/10.3389/fmicb.2022.1110151.

Wang, J., Tu, X., Zhang, H., Cui, J., Ni, K., Chen, J., Cheng, Y., Zhang, J., Chang, S.X., 2020. Effects of ammonium-based nitrogen addition on soil nitrification and nitrogen gas emissions depend on fertilizer-induced changes in pH in a tea plantation soil. The Science of the Total Environment 747, 141340. https://doi.org/10.1016/j.scitotenv.2020.141340.

Wang, X., Wolfbeis, O.S., 2014. Optical methods for sensing and imaging oxygen: materials, spectroscopies and applications. Chemical Society Reviews 43, 3666–3761. https://doi.org/10.1039/C4CS00039K.

Wolfbeis, O.S., 2015. Luminescent sensing and imaging of oxygen: fierce competition to the clark electrode. BioEssays 37, 921–928. https://doi.org/10.1002/bies.201500002.

Zhu, K., Bruun, S., Larsen, M., Glud, R.N., Jensen, L.S., 2014. Spatial oxygen distribution and nitrous oxide emissions from soil after manure application: a novel approach using planar optodes. Journal of Environmental Quality 43, 1809–1812. https://doi.org/10.2134/jeq2014.03.0125.

Zhu, K., Ye, X., Ran, H., Zhang, P., Wang, G., 2022. Contrasting effects of straw and biochar on microscale heterogeneity of soil O2 and pH: implication for N2O emissions. Soil Biology and Biochemistry 166, 108564. https://doi.org/10.1016/j.soilbio.2022.108564.

Zieger, S.E., Jones, P.D., Koren, K., 2022. Noise versus resolution in optical chemical imaging—how reliable are our measurements? ACS Omega 7, 11829–11838. https://doi.org/10.1021/acsomega.1c07232.

Zieger, S.E., Koren, K., 2023. Machine learning for optical chemical multi-analyte imaging. Analytical and Bioanalytical Chemistry 415, 2749–2761. https://doi.org/10.1007/s00216-023-04678-8.